The Canadian Mineralogist
Vol. 43, pp. 1663-1686 (2005)

NEW DATA ON "BONANZA"-TYPE PGE MINERALIZATION IN THE KIRAKKAJUPPURA PGE DEPOSIT, PENIKAT LAYERED COMPLEX, FINLAND

ANDREI Y. BARKOV[§] AND MICHAEL E. FLEET

Department of Earth Sciences, University of Western Ontario, London, Ontario N6A 5B7, Canada

ROBERT F. MARTIN

Department of Earth and Planetary Sciences, McGill University, 3450 University Street, Montreal, Quebec H3A 2A7, Canada

TAPIO A.A. HALKOAHO

Geological Survey of Finland, Regional Office for Mid-Finland, P.O. Box 1237, FIN-70211 Kuopio, Finland

ABSTRACT

Various platinum-group minerals (PGM), phases rich in the platinum-group elements (PGE), and unusual species occur in the Kirakkajuppura area, Penikat layered complex, Finland. The PGM are intimately associated with actinolite and clinochlore. The base-metal sulfides [chalcopyrite, millerite, bornite, chalcocite, ferroan chalcocite(?), digenite or roxbyite: Cu_9S_5] are in minor or trace amounts. The observed PGM and rare species are: vysotskite–braggite series [PdS–(Pt,Pd)S], zvyagintsevite [Pd_3Pb], a zvyagintsevite-like phase [$(Pd,Pt)_3(Pb,Cu)$], unnamed Pd–Pb oxide [Pd_7PbO_8 or $Pd_{3.5}Pb_{0.5}O_4$], various Cu–Fe–PGE thiospinels (large grains and unusual micro-aggregates), laflammeite [$Pd_3Pb_2S_2$], laurite–erlichmanite series [$(Ru,Os,Ir)(S,As)_2$ – $(Os,Ru,Ir)(S,As)_2$], irarsite–hollingworthite series [$(Ir,Rh,Ru)As_{1-x}S_{1+x}$ – $(Rh,Ir,Ru)As_{1-x}S_{1+x}$; $x \le 0.2$], konderite-like Pb–(Pd)-rich sulfides and a Fe-dominant analogue of konderite [$(Cu,Ni,Fe)_{3+x}(Fe,Pb)(Rh,Ir,Pd)_{8-x}S_{16}$; $x < 0.5$], unnamed $Rh_{1-x}(Ni,Fe,Cu)_{2+x}S_3$ ($0 \le x \le 0.1$), a Pd–Pt–Cu alloy [Pt-rich, Cu-rich palladium: $Pd_{89.42–91.22}Pt_{5.94–6.16}Cu_{2.62–4.64}$], skaergaardite–hongshiite [$(Pd_{0.92}Pt_{0.10})_{\Sigma 1.02}Cu_{0.98}$], keithconnite [$Pd_{20}(Te,Bi)_7$], plumbian keithconnite [$Pd_{20}(Te_6Pb)$], unnamed $Pd_5(As,Te,Sn,Pb)_2$, Pd-rich, Cu-rich gold [$Au_{76.1–81.1}Pd_{13.7–16.0}Cu_{6.1–6.3}Ag_{1.2–3.4}$], Zn-rich copper (natural?), unnamed $Pb_4O(VO_4)_2$, and an undefined Pb-rich iron silicate (hydrous?). In addition, unnamed $(Th,Ca)(V^{5+},Si,P)O_4$ and associated baddeleyite, barite, and a phosphatian huttonite or thorite occur in a pegmatitic gabbro from Kirakkajuppura. The Kirakkajuppura PGE mineralization probably formed by efficient hydrothermal remobilization and transport of PGE from their "primary" zones [Pd–Pt zones associated with the low-sulfide SJ reef and Ru–Os-mineralized chromitite zones], resulting in the local deposition of the extremely S-poor, PGE-rich assemblage, which is intimately associated with hydrous silicates and is located near the northern end of the Penikat complex.

Keywords: platinum-group elements, platinum-group minerals, hydrothermal mineralization, Kirakkajuppura deposit, Penikat layered complex, Fennoscandian Shield, Finland.

SOMMAIRE

On trouve une variété de minéraux du groupe du platine (MGP), de phases enrichies en éléments du groupe du platine (EGP), et des espèces inhabituelles dans la région de Kirakkajuppura, partie du complexe stratiforme de Penikat, en Finlande. Les MGP sont intimement associés à l'actinolite et au clinochlore. Les sulfures des métaux de base [chalcopyrite, millerite, bornite, chalcocite, chalcocite ferreuse(?), digénite ou roxbyite: Cu_9S_5] sont présents en proportions mineures ou en traces. Les MGP et espèces rares observés sont: membres de la série vysotskite–braggite [PdS–(Pt,Pd)S], zvyagintsévite [Pd_3Pb], une phase ressemblant à la zvyagintsévite [$(Pd,Pt)_3(Pb,Cu)$], un oxyde Pd–Pb sans nom [Pd_7PbO_8 ou $Pd_{3.5}Pb_{0.5}O_4$], un ensemble de thiospinelles de Cu–Fe–EGP (en gros grains ou en micro-aggrégats inhabituels), laflammeïte [$Pd_3Pb_2S_2$], membres de la série laurite–erlichmanite [$(Ru,Os,Ir)(S,As)_2$ – $(Os,Ru,Ir)(S,As)_2$], membres de la série irarsite–hollingworthite [$(Ir,Rh,Ru)As_{1-x}S_{1+x}$ – $(Rh,Ir,Ru)As_{1-x}S_{1+x}$; $x \le 0.2$], des sulfures riches en Pb et Pd ressemblant à la kondérite, et un analogue de la kondérite à dominance de Fe [$(Cu,Ni,Fe)_{3+x}(Fe,Pb)(Rh,Ir,Pd)_{8-x}S_{16}$; $x < 0.5$], $Rh_{1-x}(Ni,Fe,Cu)_{2+x}S_3$ ($0 \le x \le 0.1$) sans nom, un alliage de Pd–Pt–Cu [palladium riche en Pt et en Cu: $Pd_{89.42–91.22}Pt_{5.94–6.16}Cu_{2.62–4.64}$], skaergaardite–hongshiite [$(Pd_{0.92}Pt_{0.10})_{\Sigma 1.02}Cu_{0.98}$], keithconnite [$Pd_{20}(Te,Bi)_7$], keithconnite plombifère [$Pd_{20}(Te_6Pb)$], $Pd_5(As,Te,Sn,Pb)_2$ sans nom, or riche en Pd et en Cu, [$Au_{76.1–81.1}Pd_{13.7–16.0}Cu_{6.1–6.3}Ag_{1.2–3.4}$], cuivre zincifère (phase naturelle?), $Pb_4O(VO_4)_2$ sans nom, et un silicate de fer riche en Pb méconnu (possiblement hydraté). De plus, nous signalons la présence de $(Th,Ca)(V^{5+},Si,P)O_4$ sans nom et son association avec la baddeleyite, barite, et

§ *E-mail address*: abarkov@eps.mcgill.ca

une huttonite ou thorite phosphatée dans une pegmatite gabbroïque à Kirakkajuppura. La suite minéralisée en EGP à Kirakkajuppura se serait formée par remobilisation et transfert efficace des EGP par voie hydrothermale à partir de zones enrichies en Pd et Pt, et appauvries en sulfures et de zones de chromitite minéralisées en Ru–Os, avec comme résultat la déposition locale d'un assemblage presque dépourvu de S, enrichi en EGP, et associé aux silicates hydroxylés près de l'extrémité nord du complexe de Penikat.

(Traduit par la Rédaction)

Mots-clés: éléments du groupe du platine, minéraux du groupe du platine, minéralisation hydrothermale, gisement de Kirakkajuppura, complexe stratiforme de Penikat, bouclier fennoscandien, Finlande.

Introduction

The Kirakkajuppura platinum-group element (PGE) deposit is hosted by the Penikat complex, Finland, a mafic–ultramafic layered intrusion of Early Proterozoic age located in the Fennoscandian shield (Alapieti & Lahtinen 1986, Halkoaho *et al*. 1989a, b, 1990, Alapieti & Halkoaho 1995). This PGE deposit is highly unusual, as is discussed in this paper, on the basis of new results of mineralogical and geochemical studies (see the Appendix for a description of the analytical methods). Recent investigations have focused on various aspects of the mineralogy and crystal chemistry of several important species of platinum-group minerals (PGM) from Kirakkajuppura (Barkov *et al*. 1999a, 2000, 2002, 2004a, b). In this paper, we provide a detailed description of the platinum-group mineralogy of this extraordinary PGE deposit, and of various minerals observed in the area of Kirakkajuppura in the Penikat complex. In addition, we report new data and observations, yielding insights into the fluid-hydrothermal origin of the mineralization.

The Geology and Mineralogy of the Kirakkajuppura PGE Deposit, Penikat Layered Complex

Background information

The Penikat complex is composed of several large blocks; it is about 23 km long and 1.5–3.5 km wide, and is hosted by late Archean granitic rocks and younger tholeiitic flows, subvolcanic sills and polymictic conglomerates. The upper contact of this complex has been removed by erosion. The layered series of the complex consists of five megacyclic units: MCU I to MCU V, from the bottom to the top (Alapieti & Lahtinen 1989, Halkoaho 1993). Narrow ranges of cryptic compositional variations are observed in the layered series; enstatite varies from En_{81} (MCU I unit) to En_{70} (MCU V unit), and clinopyroxene (augite and diopside) is $Ca_{41.5–46.9}Mg_{41.6–50.5}Fe_{5.8–14.9}$, but olivine is entirely altered (Halkoaho 1993). The Kirakkajuppura PGE deposit forms part of the sulfide-poor Sompujärvi (SJ) PGE reef, located at the boundary between the MCU III and MCU IV units, or 0.5 to 1 km above the base, and extending along the entire length of the Penikat complex (Halkoaho 1993). The Kirakkajuppura deposit is situated relatively near the country rocks, at the interface of the peridotitic (pyroxenitic) and gabbroic cumulates, at the northern end of the complex (Fig. 1). Primary silicate minerals have been almost entirely replaced by hydrous silicates in the PGE-mineralized rocks; unaltered augite and diopside are preserved only in the vicinity of the PGE deposit. In the Kirakkajuppura area, accessory chromite is enriched in Al (Table 1), ilmenite is strongly enriched in Mn (up to 25 mol.% pyrophanite end-member: Table 2), apatite is poor in Cl (<0.4 wt.%) and rich in F (>2 wt.%), and phlogopite is essentially Cl-free, consistent with its high-magnesium composition [the *mg#* is in the range 61–72, where *mg#* = 100Mg:(Mg + Fe + Mn)]. The PGE mineralization is distributed highly erratically, and is not controlled in this deposit by a specific type of cumulate rock(s), pyroxenitic or gabbroic. A hydrothermally altered pyroxenite seems to be the preferred host for the PGE mineralization (up to >0.5 kg/t total PGE). This pyroxenite now consists principally of actinolite (about 70 modal %) and varying amounts of clinochlore; both of these have high values of *mg#*, about 80 and 70, respectively. Disseminated chromite (up to 10 modal %) is

TABLE 1. REPRESENTATIVE RESULTS OF ELECTRON-MICROPROBE ANALYSES OF ACCESSORY CHROMITE, KIRAKKAJUPPURA AREA

Sample	9586-5129	9585-3654	9585-3654	9585-3675	467B-PTPRO
TiO_2 wt.%	1.19	1.68	1.71	1.74	0.94
Al_2O_3	13.98	11.34	13.21	12.37	13.06
Cr_2O_3	38.24	36.13	35.38	33.99	41.94
V_2O_3	0.41	0.36	0.35	0.37	0.48
FeOt	41.74	45.60	44.38	45.17	37.09
MnO	0.99	1.90	1.58	1.29	1.81
MgO	1.29	0.31	0.50	0.68	0.47
ZnO	0.28	1.86	1.44	1.01	1.42
NiO	0.16	0.04	0.04	0.15	0.15
Sum	98.28	99.22	98.59	96.77	97.36
Fe_2O_3 §	11.09	15.88	13.95	15.16	7.45
FeO	31.77	31.32	31.83	31.53	30.39
Total	99.40	100.82	99.99	98.29	98.11
RCr_2O_4 mol.%	0.55	0.53	0.52	0.51	0.61
RAl_2O_4	0.30	0.25	0.29	0.28	0.28
Fe_3O_4	0.15	0.22	0.19	0.22	0.10

Results of WDS electron-microprobe analyses (in wt.%).
§ Calculated assuming stoichiometry.

distributed heterogeneously; it may be virtually absent in samples of PGE-rich rock, which also are nearly free of base-metal sulfide minerals. Titanite occurs as individual grains and chain-like micro-aggregates, enclosed by the hydrous silicates. Compositions of several titanite grains by SEM–EDS give the formula: $(Ca_{0.97–0.99}Fe_{0.01})(Ti_{0.98–1.00}Cr_{0–0.02})Si_{1.00–1.02}O_5$.

Base-metal sulfides

Representative compositions of various sulfide minerals present in minor or trace quantities in the Kirakkajuppura deposit are listed in Table 3; these minerals occur as small grains and intergrowths and are commonly up to 0.3 mm in size. The EMPA compositions correspond to chalcopyrite (anal. 1), millerite (anal. 2), bornite (anal. 3), chalcocite (anal. 4), which may be secondary in origin (after bornite), digenite or roxbyite: Cu_9S_5, rather than anilite: Cu_7S_4 (anal. 5), and ferroan chalcocite(?) (anal. 6, Table 3). Similar to various PGM, base-metal sulfide minerals in the Kirakkajuppura deposit may contain abundant micro-inclusions of clinochlore.

Vysotskite–braggite series [*PdS–(Pt,Pd)S*]

In general, members of the vysotskite–braggite series are the major PGM in the Kirakkajuppura deposit. Large grains of these Pd–Pt sulfides, up to 2–3 mm in size and anhedral to subhedral, are common in samples of heavy-mineral concentrates (*e.g.*, Fig. 2). Unusually long, veinlet- or chain-like aggregates of vysotskite–braggite, up to 1 cm in length (Fig. 3) and associated with zvyagintsevite, unnamed Pd–Pb oxide, and PGE thiospinels, are enclosed within the hydrous silicates (actinolite and clinochlore). Some of the vysotskite–braggite grains, present in these aggregates, seem to be oxidized and altered to various degrees. Additionally, chain-like aggregates of minute vysotskite–braggite grains (up to 5–10 μm each) are observed. A broad compositional range, based on these described varieties, is observed (Fig. 4, Table 4). Note that: (1) the vysotskite–braggite series ranges in composition from nearly end-member "PdS" to palladoan braggite, located near the compositional limit of vysotskite; (2) this series is relatively poor in Ni; the mean composition, based on a total of 60 EMP analyses (this study) of various vysotskite–braggite grains from Kirakkajuppura, is poor in Ni (0.05 atoms per formula unit, *apfu*) and rich in Pd $[(Pd_{0.74}Pt_{0.23}Ni_{0.05})_{\Sigma 1.02}S_{0.99}]$. The most Ni-rich compositions (up to 0.18 Ni *apfu*) are observed in late-stage alteration zones ("AZ": Fig. 4), developed in some of these grains (Barkov *et al*. 2004a). The Pd-rich compositions of vysotskite at Kirakkajuppura imply a low temperature of crystallization, consistent with experiments indicating that an increase in contents of Pd and Ni, with decreasing Pt contents, accompanies a lower temperature of equilibration for the vysotskite–braggite series (Cabri *et al*. 1978, Verryn & Merkle 2002); (3) Figure 5 shows compositional variations, expressed in terms of (Pd + Ni) *versus* Pt, for the vysotskite–braggite series from Kirakkajuppura; the observed slope is –1.08, so that a (Pd + Ni)-for-Pt substitution is likely combined with a Pd-for-Pt substitution. Two substitution mechanisms, $[(Pd + Ni)^{2+}=Pt^{2+}]$ and $[Pd^{2+}=Pt^{2+}]$, are also implied by the compositional zoning in Ni-rich braggite ("Brg–1" and "Brg–2" zones: Barkov *et al*. 1995) from Lukkulaisvaara, which is a neighboring layered intrusion in the Fennoscandian (Baltic) shield.

Zvyagintsevite [Pd_3Pb]

Zvyagintsevite, one of the principal PGM in the deposit, occurs in a great variety of textural forms and

TABLE 2. COMPOSITIONS OF ACCESSORY MANGANOAN ILMENITE, KIRAKKAJUPPURA AREA, PENIKAT COMPLEX

	1	2	3		1	2	3
TiO_2 wt.%	53.61	52.62	54.80	Cr *apfu*	<0.01	<0.01	0.00
V_2O_3	0.07	<0.05	<0.05	Ti	2.00	2.01	2.06
Cr_2O_3	0.11	0.20	<0.02	V	<0.01	0.00	0.00
FeOt	43.27	42.68	33.02	Mg	0.05	<0.01	<0.01
MnO	3.61	3.41	11.10	Fe^{2+}	1.79	1.81	1.38
MgO	0.60	0.11	0.10	Mn	0.15	0.15	0.47
CaO	0.16	<0.05	0.56	Ca	<0.01	0.00	0.03
NiO	<0.02	<0.02	0.03	Ni	0.00	0.00	<0.01
Total	101.43	99.01	99.62				

Column 1: sample 9585-3655; column 2: sample 9585-3664; column 3: sample 433-PTPRO. Results of WDS electron-microprobe analyses. Contents of SiO_2, Al_2O_3, Na_2O, K_2O, and ZnO are <0.05%. The atom proportions are based on six atoms of oxygen per formula unit (*apfu*).

TABLE 3. COMPOSITIONS OF BASE-METAL SULFIDE MINERALS FROM THE KIRAKKAJUPPURA PGE DEPOSIT, PENIKAT COMPLEX, FINLAND

wt.%	Cu	Fe	Ni	Co	S	Total
1	35.14	30.60	n.d.	n.d.	34.26	100.0
2	n.d.	0.24	65.32	0.40	34.92	100.9
3	62.55	12.35	n.d.	n.d.	25.11	100.0
4	79.60	n.d.	n.d.	n.d.	19.42	99.0
5	77.91	0.23	n.d.	n.d.	21.50	99.6
6	71.77	9.95	n.d.	n.d.	18.28	100.0
apfu	Cu	Fe	Ni	Co	Σ*Me*	S
1	1.02	1.01	-	-	-	1.97
2	-	<0.01	1.01	<0.01	-	0.98
3	4.95	1.11	-	-	-	3.94
4	2.02	-	-	-	2.02	0.98
5	9.03	0.03	-	-	9.06	4.94
6	1.80	0.28	-	-	2.08	0.91

Results of EDS and WDS analyses are expressed in wt.%. n.d.: not detected (<0.2 wt.%). 1: chalcopyrite; 2: millerite, 3: bornite, 4: chalcocite (probably secondary after bornite), 5: digenite or roxbyite, and 6: ferroan chalcocite(?). The atom proportions are based on a total of 4 (no. 1), 2 (no. 2), 10 (no. 3), 3 (no. 4 and 6), and 14 atoms per formula unit (no. 5).

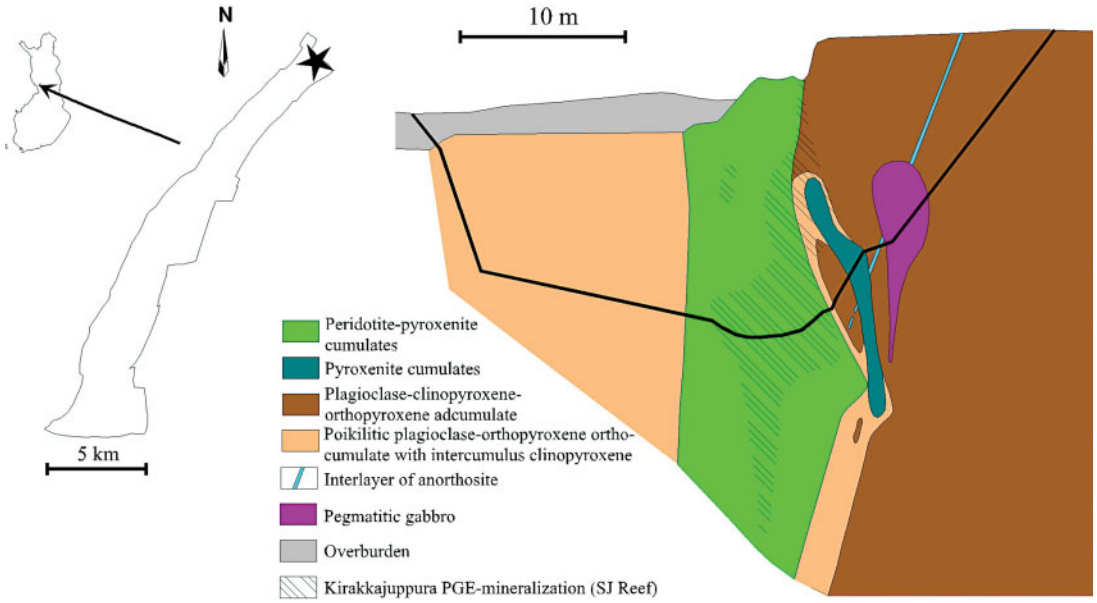

FIG. 1. Principal geological characteristics of the Kirakkajuppura PGE deposit, displayed in a cross-section through the PGE–(Au)-mineralized zone; the outline of an exploratory pit is drawn in bold (after Halkoaho *et al.* 1989b, Alapieti & Lahtinen 1989). The location of the Kirakkajuppura PGE deposit (shown by the star) in the Penikat complex, and of the Penikat complex (shown by the arrow) in Finland, are shown in the insert at the upper left.

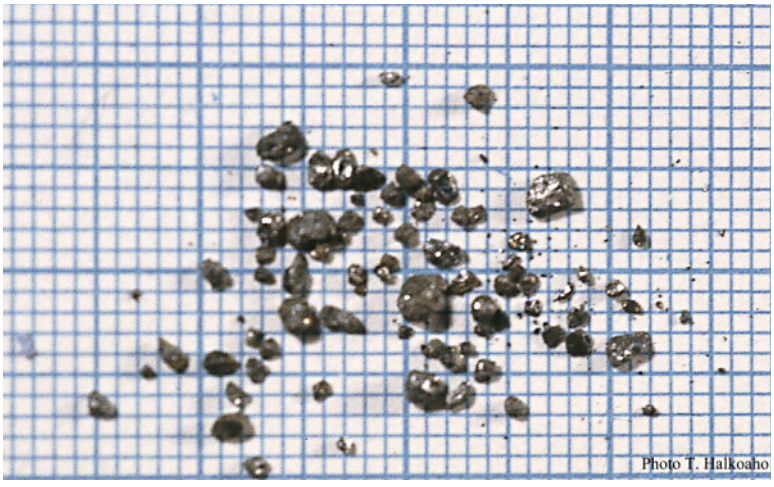

FIG. 2. An array of large grains of various platinum-group minerals from the Kirakkajuppura deposit, in a sample of heavy-mineral concentrate. Size of the net, shown for scale, equals 1 mm.

associations, as: (1) subhedral to euhedral cubic crystals, up to 0.25 mm in size (*e.g.*, Fig. 6A), (2) large anhedral and irregular grains and aggregates enclosed by actinolite and clinochlore, (3) micro-aggregates, which are commonly chain-like, with individual (subhedral or anhedral) micrograins ranging from less than 1 to 5–10 μm and finely dispersed within the hydrous silicates, (4) micro-inclusions (subhedral, anhedral, or globular)

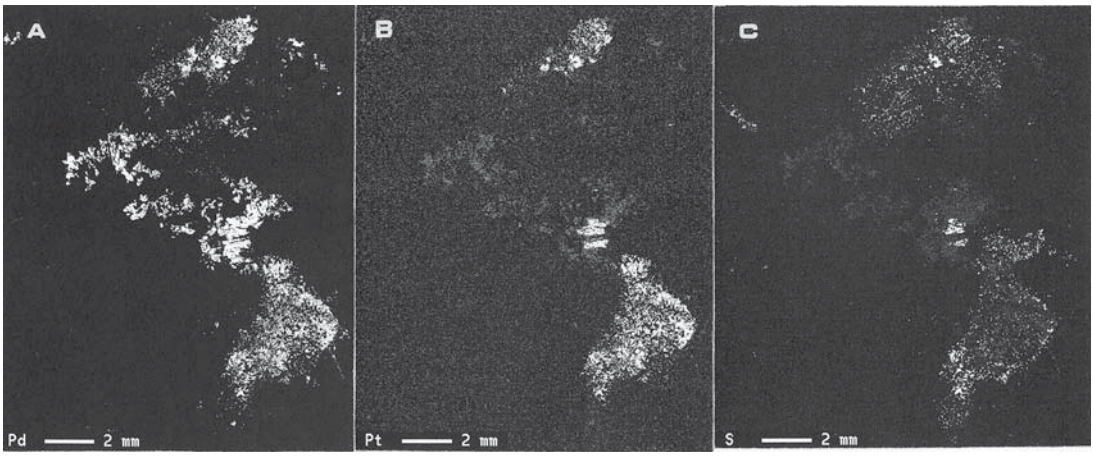

FIG. 3. Complementary X-ray maps for Pd (A), Pt (B), and S (C), showing the distribution of coarse aggregates of various platinum-group minerals (PGM), dominantly vysotskite–braggite, enclosed by hydrous silicates (actinolite and clinochlore). Note that these veinlet-like PGM aggregates reach about 1 cm in length, and that no grains of base-metal sulfide minerals are observed among these aggregates.

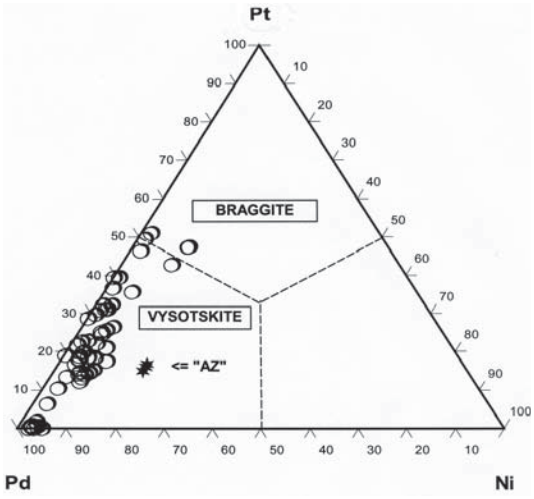

FIG. 4. Compositional variations, expressed in atoms per formula unit (*apfu*), of the vysotskite–braggite series from the Kirakkajuppura deposit, Penikat complex, in the Pd–Pt–Ni diagram. A total of 60 EMP analyses (n = 60), made on variously textured large grains and inclusions of vysotskite–braggite in other PGM, are plotted. Compositions of vysotskite from late-stage alteration zones ("AZ": most enriched in Ni) developed in some of the large vysotskite–braggite grains are shown by filled stars.

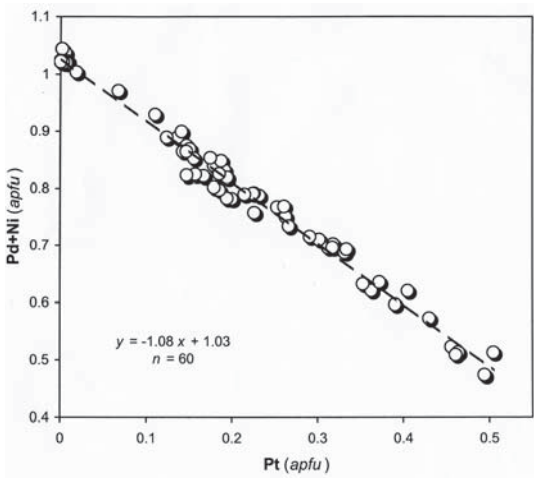

FIG. 5. Pd + Ni *versus* Pt correlation (in *apfu*: Σatoms = 2) for the vysotskite–braggite series from the Kirakkajuppura PGE deposit, Penikat complex.

in various PGM, which are especially abundant in PGE thiospinels (*e.g.*, Fig. 7B), (5) narrow veinlet-like zones of alteration in various PGM, typically in vysotskite–braggite, (6) complex intergrowths of zvyagintsevite and unnamed Pd–Pb oxide, observed as large (*ca*. 0.3 mm) or submicrometric grains, showing complementary textural relations, consistent with the formation of this Pd–Pb oxide at the expense of zvyagintsevite, or, locally, *vice versa*, with the precipitation of zvyagintsevite after the associated Pd–Pb oxide. A total of 80 zvyagintsevite grains observed in various textural associations were analyzed; they have a uniform composi-

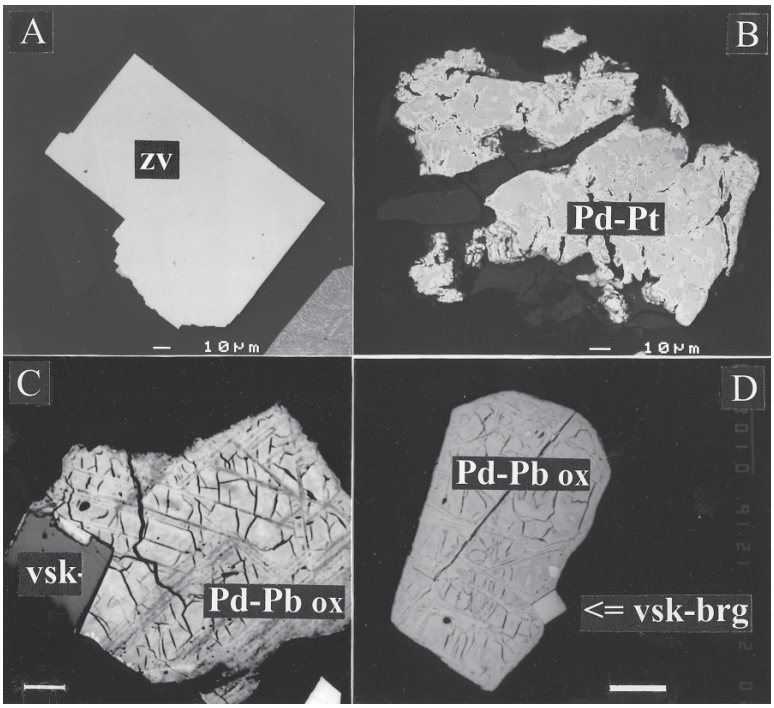

FIG. 6. A. Euhedral grain of zvyagintsevite (zv). B. Anhedral grain of a Pd–Pt alloy ("Pd–Pt"), the host for abundant microveinlets of secondary zvyagintsevite-type phases (white). C and D. Pd–Pb oxide grains ("Pd–Pb ox"), consisting of tiny grains of vysotskite (vsk) and vysotskite–braggite (vsk–brg) located at the grain boundaries. Back-scattered-electron images; the host material (black) is epoxy. The scale bar is 30 μm (C) and 50 μm (D).

tion close to end-member Pd_3Pb (Fig. 8, Table 5), with minor contents of Pt (≤2 wt.%), Cu (≤1.5 %), and Sn (≤1%). One of these grains contains elevated Sn: 4.6 wt.%, corresponding to 0.21 Sn *apfu*. The Pt and Sn are presumably incorporated as the atokite–rustenburgite component [$(Pd,Pt)_3Sn$]. Continuous solid-solution series may exist in the zvyagintsevite Pd_3Pb–unnamed Pt_3Pb–rustenburgite Pt_3Sn–atokite Pd_3Sn system, because these end members have a related structure (cubic Cu_3Au structure-type). Extensive or complete solid-solutions belonging to this system likely occur in nature; it is noteworthy that zvyagintsevite-type intermetallic compounds from Noril'sk, Siberia, contain up to 0.17 Pt *apfu* and 0.46 Sn *apfu* (Genkin *et al*. 1966, Cabri & Traill 1966).

Zvyagintsevite-like phase [$(Pd,Pt)_3(Pb,Cu)$]

A zvyagintsevite-like phase, enriched in Pt and Cu, is secondary after vysotskite–braggite, and has the following composition: Pd 55.4, Pt 10.1, Cu 2.5, Pb 32.0, Sn not detected, for a total of 100.0 wt.% (SEM–EDS data). The formula $[(Pd_{2.72}Pt_{0.27})_{\Sigma 2.99}(Pb_{0.81}Cu_{0.21})_{\Sigma 1.02}$: Σatoms = 4] is indicative of a Cu_3Au-type solid solution, and suggests that 0.2 Cu *apfu* are incorporated at the Pb site, thus replacing Pd, in contrast to the other analyzed zvyagintsevite-type compounds (Fig. 8). If so, the Cu may have entered the structure in the form of a hypothetical "$(Pd,Pt)_3Cu$" component. An ordered "Pd_3Cu" phase does not exist in the system Pd–Cu; however, a ternary $Pd_3(Cu,Ni)$ phase, having a Cu_3Au-type structure, is known (Berlincourt *et al*. 1981); the incorporation of Ni presumably exerts a stabilizing effect. The presence of Pt could be also significant in the stabilization of the hypothetical "$(Pd,Pt)_3Cu$" compound.

Revised data for unnamed Pd–Pb oxide [Pd_7PbO_8]

The unnamed Pd–Pb oxide, provisionally described as "Pd_9PbO_{10}", is anhydrous and cryptocrystalline (Barkov *et al*. 1999a). The grain size of this oxide from Kirakkajuppura varies from <10 μm to 0.3 mm. It is gray under reflected light, with very low reflectance and

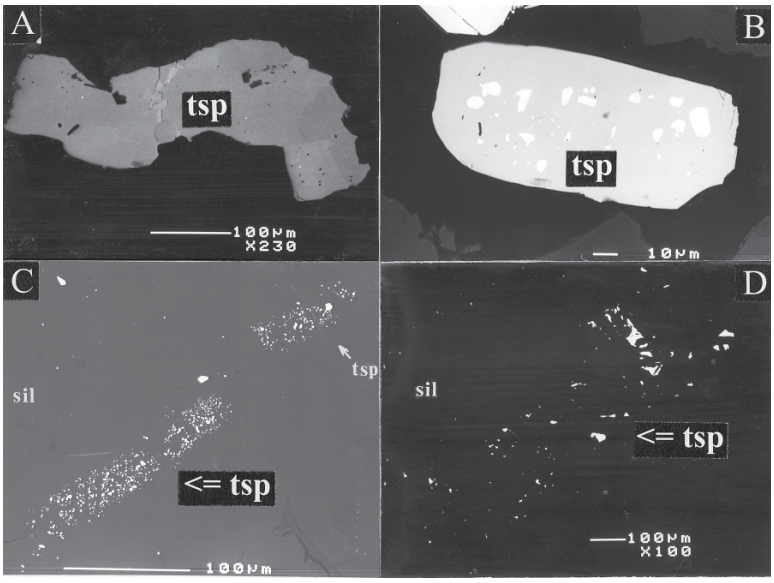

FIG. 7. A, B. Large grains of PGE thiospinel (tsp); abundant micro-inclusions of zvyagintsevite are white (B), and the host material (epoxy) is black. C, D. Unusual micro-aggregates of PGE thiospinels (tsp), in "area 1" (C) and "area 2" (D), which are enclosed within hydrous silicates (sil). Back-scattered-electron images.

TABLE 4. COMPOSITIONS OF MEMBERS OF THE VYSOTSKITE-BRAGGITE SERIES FROM THE KIRAKKAJUPPURA PGE DEPOSIT, PENIKAT COMPLEX

wt.%		Pd	Pt	Ni	S	Total
EDS	*1*	51.24	28.29	0.66	19.68	99.87
EDS	*2*	43.02	37.29	1.01	18.86	100.18
EDS	*3*	51.88	22.87	3.66	20.61	99.02
WDS	*4*	38.46	41.86	0.34	19.28	99.94
WDS	*5*	36.13	44.22	0.40	18.86	99.61
EDS	*6*	45.14	35.74	0.39	19.22	100.49
EDS	*7*	55.91	24.44	0.09	20.36	100.80
EDS	*8*	52.49	27.70	0.43	19.97	100.59
EDS	*9*	76.75	0.91	1.04	22.64	101.34
EDS	*10*	57.99	19.70	2.14	21.04	100.87
apfu		Pd	Pt	Ni	Σ*Me*	S
	1	0.77	0.23	0.02	1.02	0.98
	2	0.67	0.32	0.03	1.02	0.98
	3	0.74	0.18	0.10	1.02	0.98
	4	0.61	0.36	0.01	0.98	1.02
	5	0.58	0.39	0.01	0.99	1.01
	6	0.70	0.30	0.01	1.01	0.99
	7	0.82	0.19	<0.01	1.01	0.99
	8	0.78	0.22	0.01	1.02	0.98
	9	1.00	<0.01	0.02	1.03	0.97
	10	0.81	0.15	0.05	1.02	0.98

EDS: results of quantitative energy-dispersion analyses (SEM–EDS). WDS: results of wavelength-dispersion electron-microprobe analyses. The atom proportions are based on a total of 2 atoms per formula unit (*apfu*).

TABLE 5. COMPOSITIONS OF ZVYAGINTSEVITE FROM THE KIRAKKAJUPPURA PGE DEPOSIT, PENIKAT COMPLEX, FINLAND

		Pd	Pt	Cu	Pb	Sn	Total
1	wt.%	57.65	0.36	0.96	40.38	n.d.	99.35
2		59.09	1.58	0.26	39.27	0.57	100.77
3		57.85	3.25	n.d.	38.36	n.d.	99.46
4		59.83	0.43	n.d.	40.52	n.d.	100.78
5		58.87	0.98	n.d.	39.69	0.23	99.77
6		58.82	1.15	n.d.	39.88	n.d.	99.85
7		58.14	1.30	0.44	40.11	n.d.	99.99
8		59.22	1.22	n.d.	40.32	0.11	100.87
9		58.87	1.07	n.d.	40.13	n.d.	100.07
10		59.02	1.58	n.d.	39.78	0.32	100.70
		Pd	Pt	Cu	Σ	Pb	Sn	Pb+Sn
1	*apfu*	2.88	0.01	0.08	2.97	1.03	-	1.03
2		2.92	0.04	0.02	2.98	1.00	0.03	1.02
3		2.92	0.09	-	3.01	0.99	-	0.99
4		2.96	0.01	-	2.97	1.03	-	1.03
5		2.94	0.03	-	2.97	1.02	0.01	1.03
6		2.94	0.03	-	2.97	1.03	-	1.03
7		2.90	0.04	0.04	2.97	1.03	-	1.03
8		2.94	0.03	-	2.97	1.03	<0.01	1.03
9		2.94	0.03	-	2.97	1.03	-	1.03
10		2.93	0.04	-	2.97	1.01	0.01	1.03

Results of quantitative energy-dispersion analyses (SEM–EDS). The compositions are expressed in wt.%. n.d.: not detected (<0.2 wt.%). The atom proportions are based on a total of four atoms per formula unit (*apfu*).

anisotropy [almost isotropic: R_1 is 20.2–20.7%, and R_2 is 20.6–21.3% at 580 nm in air: reflectance values courtesy of the late A.J. Criddle, Natural History Museum, London]. Also, the following features are characteristic of this Pd–Pb oxide: (1) abundant microfractures, resembling syneresis cracks (*e.g.*, Figs. 6C, D), which likely formed because of a change in volume during oxidation; (2) cleavage-related fractures, linear and subparallel to each other, and a late alteration along other fractures, cutting the cleavage (Fig. 6C), and (3) the presence of inclusions or relics of zvyagintsevite. Also note that unaltered vysotskite–braggite grains are located at Pd–Pb oxide grain boundaries (Figs. 6C, D). These observations imply that the Pd–Pb oxide is a product of oxidation of zvyagintsevite, so that the subhedral habit of the oxide grains (*e.g.*, Fig. 6D) could be rather an expression of pseudomorphism.

Compositions of various grains of the Pd–Pb oxide are listed in Table 6. Barkov *et al*. (1999a) noted that a structural characterization of this Pd–Pb oxide is impossible owing to poor quality of the crystals. Nevertheless, the X-ray powder data obtained (Table 7; courtesy A.C. Roberts, Geological Survey of Canada, Ottawa) clearly differ from those of the tetragonal and cubic modifications of PdO (*cf*. PDF 43–1024 and 46–1211), allowing the "(Pd,Pb)O" formula to be dismissed. High levels of Pb are invariably observed in the Pd–Pb oxide (Table 6), implying the existence of a specific Pb site in the crystal structure.

A revision of the preliminary "Pd_9PbO_{10}" formula is suggested in Table 6. The revised formula: $Pd^{2+}{}_7Pb^{2+}O_8$ or $Pd^{2+}{}_{3.5}Pb^{2+}{}_{0.5}O_4$ is based on a general similarity of the X-ray powder pattern of this Pd–Pb oxide (Table 7) with the following pattern reported for synthetic Pd_3SrO_4 (or $SrPd_3O_4$) [*d* in Å (I)]: 2.606 (100), 2.378 (70), 2.059 (<5), 1.842 (<5), 1.682 (20), 1.616 (30), 1.557 (40), 1.457 (25), and 1.303 (5), consistent with cubic symmetry, *a* 5.826 Å, and space group is *Pm*3*n* (ICDD 23–1299). Synthetic Pd_3SrO_4 is black in color; it has a cubic $Na_xPt_3O_4$-type structure, space group *Pm*3*n*, with *Z*=2 and *a* 5.8120(7) Å, in common with the other MPd_3O_4 ternary palladates; *M* = Sr, Ca, Cd (Wasel-Nielen & Hoppe 1970, Muller & Roy 1971, Smallwood *et al*. 2000). Interestingly, synthetic $Na_xPt_3O_4$ is microcrystalline, similar to the Pd–Pb oxide mineral from Kirakkajuppura. The Na content varies from 0 to 1 *apfu* in the synthetic $Na_xPt_3O_4$ phase, and the Na ions are located in holes, which are formed by cubic clusters of O atoms (Waser & McClanahan 1952).

Interestingly, for Na=1 *apfu*, the Pt ions presumably have a mixed-valence state in synthetic $Na_xPt_3O_4$, so that the corresponding formula is $[Na^{+}Pt^{2+}{}_{2.5}Pt^{4+}{}_{0.5}O_4]$, with an atomic Pt^{2+}:Pt^{4+} ratio of 5. By analogy with this prototype phase, and also with synthetic $Pd^{2+}{}_3Sr^{2+}O_4$, the mean composition of the Pd–Pb oxide from Kirakkajuppura may correspond to a formula of $Pd^{2+}{}_{3.5}Pb^{2+}{}_{0.5}O_4$, based on 4 oxygen atoms. Note that: (1) 0.5 Pb^{2+} *apfu* in the Pd–Pb oxide formula gives

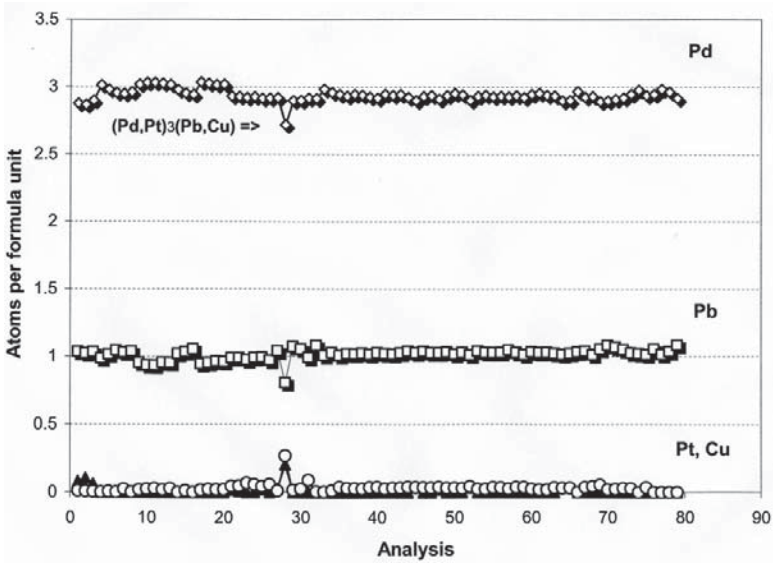

FIG. 8. Proportions of Pd (open diamond), Pb (open square), Pt (open circle), and Cu (filled triangle), in atoms per formula unit calculated on the basis of Σatoms = 4; results of 80 EMP analyses of zvyagintsevite (this study) from the Kirakkajuppura deposit, Penikat complex, are plotted.

one positive charge and corresponds to 1 Na^+ *apfu* in the formula of $Na^+Pt^{2+}_{2.5}Pt^{4+}_{0.5}O_4$; (2) the Pb content may well vary to some degree consistent with the behavior of Na in synthetic $Na_xPt_3O_4$. On the other hand, in spite of the superficial similarity, the XRD pattern obtained for the Pd–Pb oxide (Table 7) is not fully indexed by the cubic Pd_3SrO_4-type cell. Thus, these Pd-rich oxides are closely related, and they are not necessarily isostructural. Also, the compositions in Table 6 suggest that variations in Pb are limited, so that Pb^{2+} could fully occupy a specific site in the structure, analogous to Sr^{2+} in synthetic Pd_3SrO_4. This reasoning suggests the alternative formula $Pd^{2+}_7Pb^{2+}O_8$. Although all Pt is listed as PtO_2 in Table 6, the presence of Pt^{2+} is also possible, analogous to the $[Na^+Pt^{2+}_{2.5}Pt^{4+}_{0.5}O_4]$ phase and the presence of Pt^{2+}, Pd^{2+} and Cu^{2+} in synthetic $(Bi,Pb)_2MO_4$ (*M*=Pd, Pt, and Cu; Bettahar *et al*. 1992).

If indexed on the basis of a tetragonal Pd_3SrO_4-derivative cell, the X-ray powder data for the Pd–Pb oxide (Table 7) correspond to: $a = 6.12$ and $c = 5.60$ Å, assuming $Z = 1$ for Pd_7PbO_8 and a calculated density of about 8.5 g/cm^3. Because of the poor X-ray-diffraction characteristics and the lack of suitable single crystals, these results are clearly preliminary and will require additional characterization.

Minute grains of the Pd–Pb oxide (≤10 μm), forming part of a chain-like PGM micro-aggregate, display elevated Cu contents (up to 4 wt.% CuO: anal. 11, 12, Table 6). Presumably, Cu^{2+} can readily substitute for Pd^{2+} (and Pt^{2+}) in various Pd–Pt-rich oxides, such as synthetic Bi_2PdO_4, $(Bi,Pb)_2(Pd,Pt)O_4$ (Bettahar *et al*. 1992), or "palladinite" [(Pd,Cu)O] from Brazil (up to 8.4 wt.% CuO: Olivo & Gauthier 1995).

We suggest that the observed Cu enrichment (0.5 Cu^{2+} *apfu*: Table 6) may point to the existence of a limited solid-solution series, extending from $Pd^{2+}_7Pb^{2+}O_8$ toward a murdochite-type $Cu^{2+}_6Pb^{4+}O_8$ oxide; the coupled charge-balance substitution is: $(7Pd^{2+} + Pb^{2+}) = (6Cu^{2+} + Pb^{4+})$. Murdochite has a cubic (*Fm*3*m*) structure, formed of Cu^{2+} ions and $[PbO_8]$ cubes; note that the "Cu_6PbO_8" formula corresponds to $x = 0$ for the general formula of murdochite, $Cu_6PbO_{8-x}(Cl,Br)_{2x}$, with $x \leq 0.5$ (Dubler *et al*. 1983, Winkler *et al*. 2000).

TABLE 6. COMPOSITIONS OF UNNAMED Pd_7PbO_8 FROM THE KIRAKKAJUPPURA PGE DEPOSIT, PENIKAT COMPLEX, FINLAND

wt.%		PdO	PtO_2	CuO	FeO	PbO	Total
WDS	*1*	79.64	n.d.	n.d.	n.d.	21.40	101.04
WDS	*2*	83.32	0.05	n.d.	n.d.	17.36	100.73
WDS	*3*	81.91	0.12	n.d.	n.d.	17.44	99.47
WDS	*4*	80.29	0.19	n.d.	n.d.	18.11	98.59
WDS	*5*	81.14	0.50	n.d.	n.d.	16.11	97.75
WDS	*6*	81.32	0.38	n.d.	n.d.	16.17	97.87
WDS	*7*	83.19	0.41	n.d.	n.d.	17.46	101.06
WDS	*8*	83.09	n.d.	n.d.	n.d.	18.98	102.07
WDS	*9*	79.86	n.d.	n.d.	n.d.	19.10	98.96
WDS	*10*	82.85	n.d.	n.d.	n.d.	18.89	101.74
EDS	*11*	72.07	0.42	3.99	2.09	21.62	100.19
EDS	*12*	73.30	1.66	3.60	1.55	19.48	99.59
apfu		Pd^{2+}	Pt^{4+}	Cu^{2+}	Fe^{2+}	Σ*Me*	Pb^{2+}
	1	6.97	–	–	–	6.97	1.03
	2	7.18	<0.01	–	–	7.18	0.82
	3	7.15	<0.01	–	–	7.16	0.84
	4	7.10	0.01	–	–	7.11	0.88
	5	7.17	0.02	–	–	7.20	0.78
	6	7.18	0.02	–	–	7.20	0.78
	7	7.14	0.02	–	–	7.16	0.82
	8	7.11	–	–	–	7.11	0.89
	9	7.07	–	–	–	7.07	0.93
	10	7.11	–	–	–	7.11	0.89
	11	6.13	0.02	0.52	0.30	6.97	1.01
	12	6.24	0.08	0.47	0.22	7.01	0.91

WDS: results of wavelength-dispersion electron-microprobe analyses; EDS: results of quantitative energy-dispersion analyses (SEM–EDS). Numbers 1–7: JEOL electron microprobe; 8–10: Cameca Camebax electron microprobe. Compositions 1–10 refer to large grains of the Pd–Pb oxide. Compositions 11 and 12 refer to tiny grains, which form part of chain-like micro-aggregates, and are enclosed within hydrous silicates. n.d.: not detected. The atom proportions are calculated on the basis of 8 oxygen atoms per formula unit (*apfu*).

Various Cu–Fe–PGE thiospinels: large grains and unusual micro-aggregates

PGE-rich thiospinels are relatively common in the Kirakkajuppura deposit. They typically occur as large grains (0.1–0.35 mm across: Figs. 7A, B), which vary strongly in composition to form extensive series of the cuprorhodsite $[CuRh_2S_4]$–ferrorhodsite $[(Fe,Cu)(Rh,Pt,Ir)_2S_4]$–cuproiridsite $[CuIr_2S_4]$ and cuprorhodsite–ferrorhodsite–malanite $[Cu(Pt,Ir,Rh)_2S_4]$ solid solutions. The Fe-rich end-member observed at Kirakkajuppura corresponds to $(Fe^{3+}_{0.5}Cu^+_{0.5})Rh^{3+}_2S^{2-}_4$ with Fe incorporated *via* the coupled charge-balance substitution $[^AFe^{3+}+2^BRh^{3+} = {}^ACu^+ + 2^BPt^{4+}(+ 2Ir^{4+})]$ (Barkov *et al*. 2000].

Interestingly, the PGE-rich thiospinels also are present as unusual micro-aggregates (*e.g.*, "area 1" in Fig. 7C and "area 2" in Fig. 7D), consisting of up to several hundreds of individual micrograins (≤5 μm each), enclosed within the host hydrous silicates. The EMP data (Table 8) and color X-ray maps (Fig. 9)

TABLE 7. X-RAY POWDER-DIFFRACTION DATA FOR UNNAMED Pd_7PbO_8 FROM THE KIRAKKAJUPPURA PGE DEPOSIT

I (est.)	d_{meas} (Å)	d_{calc} (Å)	*hkl*	I (est.)	d_{meas} (Å)	d_{calc} (Å)	*hkl*
10 *b*	2.690	2.685	201	1 *b*	1.550	1.542	213
3	2.350	2.351	112	1	1.440	1.443	330
0.5	2.170	2.164	220			1.435	411
1	2.040	2.040	300	1 *b*	1.330	1.332	114
0.5	1.820	1.829	311			1.329	421
1 *b*	1.680	1.697	320				

This pattern was obtained courtesy of A.C. Roberts; the analytical conditions are given in Barkov *et al.* (1999a); *b* broad line.

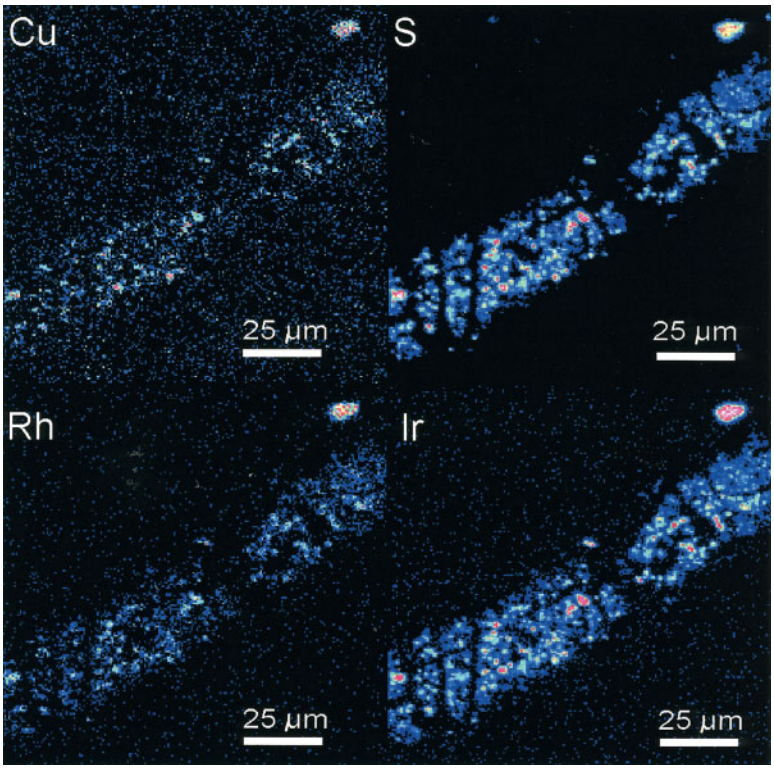

FIG. 9. The color X-ray maps for Cu (Cu), S (S), Rh (Rh), and Ir (Ir), showing the distribution of minute grains of PGE thiospinel (tsp) from micro-aggregate in "area 1" (shown by arrow in Fig. 7C) enclosed within actinolite. Note that these thiospinel grains appear compositionally uniform, in spite of the change in color (from red to blue and dark blue), observed locally in these maps.

are consistent with a monomineralic character of these micro-aggregates; no PGM other than PGE-rich thiospinels were observed. Results of multiple EMP analyses indicate that the "area 1" and "area 2" micrograins of thiospinel are compositionally distinct, and correspond to *cuproiridsite* and *cuprorhodsite*, respectively (Table 8, Fig. 10). The "area 2" thiospinel is more closely stoichiometric (relative to ideal AB_2S_4); the grains are richer in Fe, Ni and Rh, and are poorer in Ir than in "area 1", in which grains display a relative excess at the *A* site (up to 1.2 *apfu*) and corresponding deficit at the *B* site (1.8 *apfu*: Table 8). All of these micrograins are characteristically poor in Pt (and in end-member malanite), in contrast to most of the larger-grain-size PGE thiospinels (Fig. 10). However, the "area 2" grains are close in composition to some of the Pt-poor "large grains" (Fig. 10), implying uniform conditions of crystallization. Also, note that the "large grains" and micro-aggregates of PGE thiospinels have distinctly different Ni contents, <0.25 and up to 2.3 wt.% Ni, respectively (Table 8).

Laflammeite [$Pd_3Pb_2S_2$]

The Kirakkajuppura area of the Penikat complex is the type locality and, to date, the only reported locality for laflammeite, which has a parkerite-type structure (Barkov *et al*. 2002). Laflammeite occurs as subhedral grains, platelets (0.2–0.3 mm) and, less commonly, anhedral grains with a perfect cleavage (Fig. 11B), and is most closely associated with vysotskite–braggite. The compositions obtained in the present study (EMPA–WDS) are consistent with an ideal $Pd_3Pb_2S_2$ formula: Pd 39.74 and 39.21, Ir 1.01–1.06, Pt <0.1, Rh <0.1, Pb 51.70 and 51.66, S 7.83 and 7.86, total 100.28 and 99.79 wt.%, corresponding to $[(Pd_{2.97–3.00}Ir_{0.04})_{\Sigma 3.01–3.04}Pb_{2.00–2.01}S_{1.96–1.98}]$.

Laurite–erlichmanite series [(Ru,Os,Ir)(S,As)$_2$ – (Os,Ru,Ir)(S,As)$_2$], and micro-inclusions of zoned laurite–erlichmanite

In the Kirakkajuppura deposit, laurite–erlichmanite occurs in a variety of textural forms, including: (1) unusually large subhedral to euhedral grains (up to 0.3 mm), which are strongly or slightly zoned, (2) cores of complexly zoned grains or of polymineralic PGM intergrowths, which are mantled by irarsite–hollingworthite, and (3) zoned micro-inclusions (<50 μm) in vysotskite–braggite (*e.g.*, Fig. 11A). Figure 12 shows that considerable compositional variation is observed in the laurite–erlichmanite series in this deposit (this study, and Barkov *et al*. 2004a), which ranges from a low-Os laurite to ruthenoan erlichmanite, located at the laurite–erlichmanite boundary. Sympathetic covariations of minor Ir, Rh, Fe, and As, and an As-for-S substitution, are characteristic of this series. Commonly, but not necessarily, the incorporation of Ir and Rh in the laurite–erlichmanite is controlled by As, as is indicated by the strong positive correlation observed for (Ir + Rh) *versus* As (Fig. 13). Barkov *et al*. (2004a) have suggested various charge-balance mechanisms responsible for the incorporation of Ir and Rh in laurite–erlichmanite at Kirakkajuppura: $[(Ir + Rh)^{3+} + (AsS)^{3-} = (Ru + Os)^{2+} + (S_2)^{2-}]$; for essentially As-free grains: $[0.67\ Ir^{3+} + 0.33\ ^{Me}\square = (Ru + Os)^{2+}]$, or $[0.52\ Ir^{3+} + 0.22\ Ir^{2+} + 0.26\ ^{Me}\square = (Ru + Os)^{2+}]$, and $[0.67\ Rh^{3+} + 0.33\ ^{Me}\square = (Ru + Os)^{2+}]$, or $[0.4\ Rh^{3+} + 0.4\ Rh^{2+} + 0.2\ ^{Me}\square = (Ru + Os)^{2+}]$. Thus, the limited nature of the solid solutions of $(Ru,Os)S_2$ with "$Ir_{1-x}S_2$" and "$Rh_{1-x}S_2$" is inferred, and is likely a result of vacancy-type defects and of related complications arising from the incorporation of Ir and Rh.

A laurite micro-inclusion shown in Figure 11A is in intimate intergrowth with a PGE thiospinel, malanite–cuprorhodsite of composition $Cu_{1.05}(Pt_{1.02}Rh_{0.92}Ir_{0.08})_{\Sigma 2.02}S_4$ (SEM/EDS: this study). This grain of laurite is compositionally zoned, with a core-like zone of $(Ru_{0.74}Os_{0.15}Ir_{0.12}Fe_{0.01})_{\Sigma 1.02}S_{1.98}$ and a rim-like zone of $(Ru_{0.83}Os_{0.13}Ir_{0.07}Fe_{0.01})_{\Sigma 1.04}S_{1.97}$. The host of these inclusions is an intermediate member of the vysotskite–braggite series $[(Pd_{0.50}Pt_{0.50}Ni_{0.01})_{\Sigma 1.01}S_{0.98}]$. The intergrowth relationships (Fig. 11A) imply that this "laurite+PGE thiospinel" inclusion could have formed by fractional crystallization of a trapped fluid or liquid. Probably, Ru and Os were "incompatible" components with respect to the thiospinel, and they were thus selec-

TABLE 8. SELECTED RESULTS OF ELECTRON-MICROPROBE ANALYSES OF PGE-RICH THIOSPINELS FROM THE "AREA 1" AND "AREA 2" MICRO-AGGREGATES ENCLOSED IN HYDROUS SILICATES, KIRAKKAJUPPURA DEPOSIT

	Cu	Fe	Ni	Rh	Ir	Co	Pt	S	Total
					"Area 1" (wt.%)				
1	12.07	0.72	0.92	8.68	48.21	0.37	0.89	25.18	97.04
2	12.09	0.78	0.92	8.47	48.35	0.51	0.61	24.78	96.51
3	12.23	0.52	0.82	8.64	48.59	0.26	0.37	24.60	96.03
4	12.31	0.71	0.79	8.84	48.65	0.38	0.27	24.51	96.46
					"Area 2"				
5	12.48	1.41	2.32	49.21	1.85	0.34	0.04	32.35	100.26
6	11.28	2.85	1.12	44.70	6.53	0.41	0.22	31.40	98.76
7	11.93	2.52	1.22	45.25	6.44	0.33	0.32	31.78	100.08
8	11.31	2.20	2.22	51.16	n.d.	0.22	0.04	32.56	99.93
9	12.00	2.40	1.44	46.82	4.20	0.38	0.05	31.98	99.50

	Cu	Fe	Ni	S	Rh	Ir	Co	Pt	Σ	S
					"Area 1" (Σ = 7 *apfu*)					
1	0.99	0.07	0.08	1.14	0.44	1.30	0.03	0.02	1.79	4.07
2	0.99	0.07	0.08	1.14	0.43	1.31	0.04	0.02	1.80	4.04
3	1.02	0.05	0.07	1.14	0.44	1.33	0.02	0.01	1.80	4.05
4	1.02	0.07	0.07	1.16	0.45	1.33	0.03	<0.01	1.82	4.02
					"Area 2"					
5	0.78	0.10	0.16	1.04	1.90	0.04	0.02	<0.01	1.96	4.00
6	0.73	0.21	0.08	1.02	1.78	0.14	0.03	<0.01	1.96	4.02
7	0.76	0.18	0.08	1.02	1.78	0.14	0.02	<0.01	1.96	4.01
8	0.70	0.16	0.15	1.01	1.96	<0.01	0.01	<0.01	1.98	4.01
9	0.76	0.17	0.10	1.03	1.83	0.09	0.03	<0.01	1.96	4.01

Results of WDS electron-microprobe analyses. The "Area 1" and "Area 2" micro-aggregates are shown in Figures 7C and D, respectively. Totals of the analyses 5–10 ("Area 2") include 0.23–0.28 wt.% Pd (<0.01 *apfu* Pd).

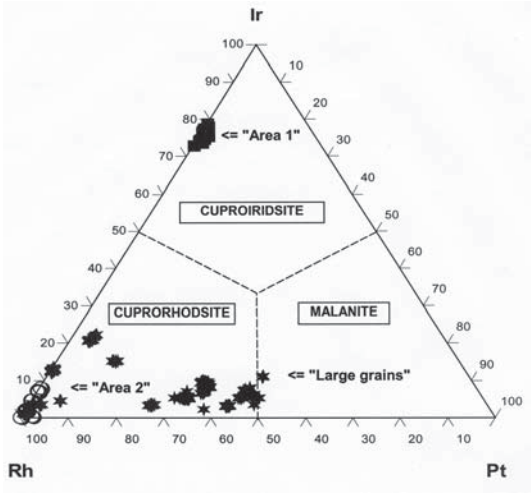

FIG. 10. Compositions of various Cu–Fe–PGE thiospinels from the Kirakkajuppura deposit in Rh–Ir–Pt compositional space (in *apfu*). Filled stars: large grains, 0.1–0.35 mm in size, members of cuprorhodsite – (ferrorhodsite) – cuproiridsite – malanite series (results of 424 EMP analyses: $n = 424$, made on 25 grains). Filled squares: minute grains ($n = 22$: up to 10 μm) from the micro-aggregate in "area 1", shown in Figure 7C. Open circles: minute grains ($n = 14$: up to 15 μm) from the micro-aggregate in "area 2", shown in Figure 7D.

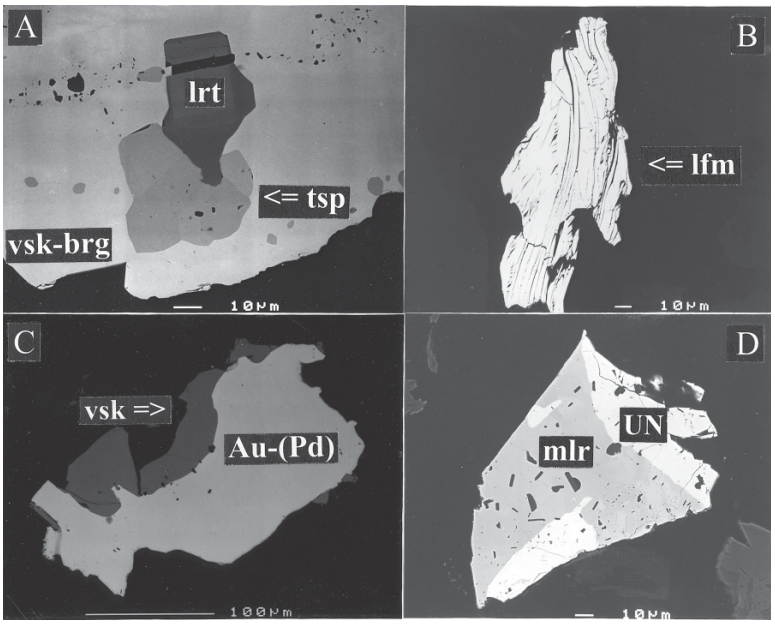

FIG. 11. A. A micro-inclusion of compositionally zoned laurite (lrt), observed in intimate intergrowth with a PGE thiospinel (tsp), hosted by a large grain of vysotskite–braggite (vsk–brg). B. Anhedral grain of laflammeite (lfm), displaying a well-developed cleavage. C. A large grain of Cu- and Pd-rich gold ["Au–(Pd)"], partly mantled by vysotskite (vsk). D. A subhedral intergrowth of millerite (mlr) with unnamed $Rh_{1-x}(Ni,Fe,Cu)_{2+x}S_3$ (UN). The minute micro-inclusions (black) present in the millerite consist of clinochlore. Back-scattered-electron images; the host material (black) is epoxy.

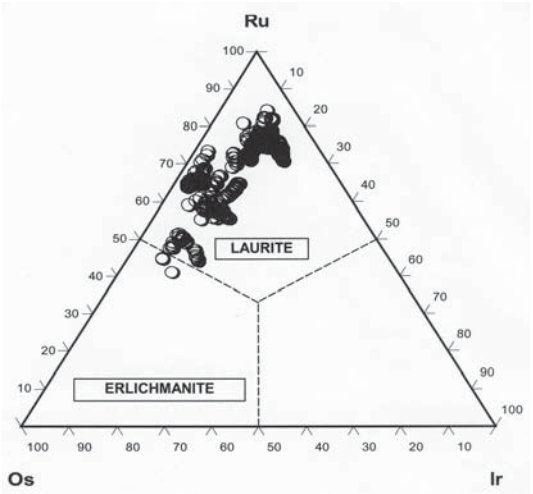

FIG. 12. Compositional variations, expressed in *apfu*, of the laurite–erlichmanite series in the Kirakkajuppura deposit, Penikat complex, in terms of the Os–Ru–Ir diagram. Results of multiple EMP analyses (n = 528) are plotted.

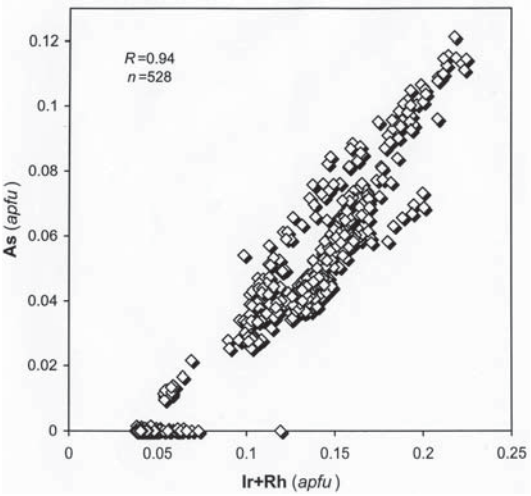

FIG. 13. As *versus* Ir + Rh correlation (in *apfu*: Σatoms = 3) for the laurite–erlichmanite series from the Kirakkajuppura deposit, Penikat complex (n = 528).

tively partitioned into the growing laurite; then, the associated thiospinel crystallized from the remaining liquid enriched in Cu–Pt–Rh, which are essentially "incompatible" in laurite.

Irarsite–hollingworthite series [$(Ir,Rh,Ru)As_{1-x}S_{1+x}$ – $(Rh,Ir,Ru)As_{1-x}S_{1+x}$, *where* $x \leq 0.2$]

Typically, irarsite–hollingworthite occurs as a rim-like zone (up to 50 μm thick), containing about 0.1 Ru *apfu* and developed around a subhedral laurite–erlichmanite core (Barkov *et al*. 2004a). The Ir content of such rims decreases outward, rapidly and antipathetically with Rh and also with minor Fe. In contrast, values of the *ir#* index [*i.e*., 100 Ir:(Ir + Rh), *in apfu*] gradually decrease toward the margin (*cf*. Barkov *et al*. 1999b), and this is thus a useful evolutionary indicator. The Ru is likely incorporated as a laurite component in the zoned irarsite–hollingworthite, dominantly by a Ru-for-Rh substitution *via* the substitution scheme: $Ru^{2+} + (S_2)^{2-} = Me^{3+} + (AsS)^{3-}$. Minor Fe, which is present as the arsenopyrite component, is likely incorporated *via* the following mechanism: $[(Rh + Fe)^{3+} = Ir^{3+}]$ (Barkov *et al*. 2004a).

Konderite-like Pb–(Pd)-rich sulfides, and an unnamed Fe-dominant analogue of konderite [$(Cu,Ni,Fe)_{3+x}(Fe,Pb)(Rh,Ir,Pd)_{8-x}S_{16}$, *where* $x < 0.5$]

A complex Pb–(Pd)-rich sulfide solid-solution, with atom proportions (Cu + Fe + Pb + Ni):(Rh + Ir + Pd + Pt + Co):S of 1:2:4, occurs as grains up to 0.15 mm in size, in a close association with the PGE thiospinels. In contrast to other chalcogenide compounds, it contains Pb (up to 9.7 wt.%) and Pd (6.4 wt.%), which covary sympathetically (Barkov *et al*. 2004b). The observed Fe-rich compositions likely correspond to an Fe-dominant analogue of konderite. The approximate scheme of coupled substitution operating in these konderite-type sulfides is $Cu^{+} + 2(Pb + Ni)^{2+}] + 2Pd^{2+} = 2Fe^{3+} + Rh^{3+}$ (Barkov *et al*. 2004b). Konderite is hexagonal, a thiospinel derivative, and reported only from the Konder Uralian–Alaskan-type complex, northeastern Russia (Rudashevsky *et al*. 1984); compositions of konderite are consistent with a structural formula of $Cu^{+}{}_3Pb^{2+}[Rh^{3+}{}_3Ir^{3+}{}_2Pt^{4+}{}_3]S^{2-}{}_{16}$ (Barkov *et al*. 2004b).

Unnamed $Rh_{1-x}(Ni,Fe,Cu)_{2+x}S_3$ $(0 \leq x \leq 0.1)$

A complex Rh–Ni–Fe–Cu chalcogenide, which may also represent a potentially new PGM species, is closely associated with millerite at Kirakkajuppura (Fig. 11D). Under reflected light, this chalcogenide has a gray color, a moderate reflectance, lower than that of millerite, and appears to display a very weak anisotropy with a slight reflection pleochroism in grayish and lilac-brownish tints. Results of the EMPA–WDS and SEM–EDS analyses of this chalcogenide are in excellent agreement; Rh, Ni, Fe, Cu are the principal constituents, whereas Ir and Co are minor, giving a Σ*Me*:S ratio of 1.00 (Table 9). This chalcogenide phase is compositionally distinct from various Rh–Ir–Pt thiospinels and konderite-like sulfides (Fig. 14), and also from pentlandite-type phases, such as $Rh(Ni_4Fe_4)S_8$, synthesized at 700°C by Knop *et al*. (1976), or $Rh(Fe_5Ni_3)S_8$, reported from Yubdo, Ethiopia (Cabri *et al*. 1996). Also, the Kirakkajuppura phase appears distinct from rhodian pyrrhotite found in Colombia, which is relatively metal-deficient: $[(Fe_{0.55-0.65}Rh_{0.18-0.26}Cu_{0.05-0.07}Ni_{0.02})\Sigma_{0.93-0.95}S_{1.05-1.07}$: Cabri *et al*. 1996)]. Results of synthesis indicate that up to 40 wt.% Rh can be incorporated in pyrrhotite at 750°C (quoted in Berlincourt *et al*. 1981). Phases of a "(Rh,Fe,Ni)S"-type, with a Σ*Me*:S ratio of about 1.0, and varying atomic proportions of the metals, have been reported from Ethiopia (Cabri *et al*. 1996).

We suggest that the phase from Kirakkajuppura has a "AB_2X_3"-type (cubanite- or isocubanite-like) stoichiometry: *i.e*., $Rh_{1-x}(Ni,Fe,Cu)_{2+x}S_3$, with $0 \leq x \leq 0.1$ (Table 9). A slight departure from ideal $(Rh,Ir)(Ni,Fe,Cu)_2S_3$ is clearly indicated by the two analytical methods (WDS and EDS), which consistently imply that minor amounts of Cu, Fe, or Ni are likely incorporated at the Rh site. This feature may be somewhat similar to that observed for the cuprorhodsite-type thiospinel $[CuRh_2S_4]$, displaying a deficit in Rh with a relative Cu excess, due to a Cu-for-Rh substitution. We thus suggest that the Kirakkajuppura phase is likely the Rh-dominant $[Rh_{1-x}(Ni,Fe,Cu)_{2+x}S_3]$ counterpart of the unnamed $(Ir,Rh)(Ni,Fe,Cu)_2S_3$, reported from chromitite occurrences associated with the ultramafic Finero complex, Italy (Garuti *et al* 1995), the Ojen lherzolite complex, Spain (Torres-Ruiz *et al*.

TABLE 9. COMPOSITION OF UNNAMED $Rh_{1-x}(Ni,Fe,Cu)_{2+x}S_3$ FROM THE KIRAKKAJUPPURA PGE DEPOSIT, PENIKAT COMPLEX, FINLAND

		Cu	Fe	Ni	Co	Rh	Ir	S	Total
WDS	*1*	7.83	8.50	21.66	0.42	29.32	1.26	30.51	99.50
WDS	*2*	7.74	8.17	21.57	0.45	29.83	1.12	30.30	99.18
EDS	*3*	7.83	8.20	21.73	0.34	29.95	1.29	31.02	100.36

Basis of recalculation: 2 *apfu*

	Cu	Fe	Ni	Co	Rh	Ir	Σ*Me*	S
1	0.13	0.16	0.39	<0.01	0.30	<0.01	1.00	1.00
2	0.13	0.16	0.39	<0.01	0.31	<0.01	1.00	1.00
3	0.13	0.15	0.39	<0.01	0.30	<0.01	0.99	1.01

Basis of recalculation: 6 *apfu*

	Cu	Fe	Ni	Co	Σ	Rh	Ir	Σ*Me*	S
1	0.39	0.48	1.17	0.02	2.06	0.90	0.02	2.99	3.01
2	0.39	0.47	1.17	0.02	2.05	0.92	0.02	2.99	3.01
3	0.39	0.46	1.16	0.02	2.03	0.91	0.02	2.96	3.04

WDS: results of wavelength-dispersion electron-microprobe analyses; EDS: result of quantitative energy-dispersion analysis (SEM–EDS).

1996), and the Oman ophiolite complex (Ahmed & Arai 2003).

Pd–Pt–Cu alloy (*Cu- and Pt-rich variety of palladium*)

A rare alloy of the Pd–Pt–Cu system occurs as small irregular grains 0.1 mm across (Fig. 6B), having the following SEM–EDS composition: Pd 86.91 and 86.87, Pt 10.59 and 10.76, Cu 2.69 and 1.49, total 100.19 and 99.12 wt.%, respectively. This alloy is thus strongly Pd-dominant and corresponds to the mineral *palladium*: [$Pd_{89.42–91.22}Pt_{5.94–6.16}Cu_{2.62–4.64}$, in at.%]. Botryoidal alloys of Pd and Pt were formed by hydrothermal alteration of mafic–ultramafic rocks at Minas Gerais, Brazil (Fleet *et al*. 2002).

Skaergaardite–hongshiite [(*Pd,Pt*)*Cu*]

Skaergaardite, PdCu, is a newly reported species of PGM discovered in the Skaergaard intrusion, East Greenland; it has a CsCl-type structure, and is isostructural with wairauite (CoFe) and related to hongshiite, PtCu (Rudashevsky *et al*. 2004). Skaergaardite is a very rare PGM at Kirakkajuppura, and was observed only as narrow alteration-induced zones (≤ 5–10 μm thick), hosted by a Pd–Pt–(Cu) alloy grain. A representative composition of skaergaardite from Kirakkajuppura (SEM–EDS data) is: Pd 54.66, Cu 34.59, Pt 11.10, Pb and Sn not detected, and total 100.35 wt.%, corresponding to the formula $(Pd_{0.92}Pt_{0.10})_{\Sigma 1.02}Cu_{0.98}$, consistent with solid solution toward hongshiite (*ca*. 10 mol.%).

Recently, a new occurrence of hongshiite has been reported, from sulfide-free and hematite-rich "jacutinga" mineralization, Minas Gerais, Brazil (Kwitko *et al*. 2002). There appear to be clear environmental similarities between this occurrence of hongshiite and that of skaergaardite–hongshiite at Kirakkajuppura, because both are associated with S-poor and highly oxidized environments.

Keithconnite [$Pd_{20}(Te,Bi)_7$], *and a plumbian variety of keithconnite* [$Pd_{20}(Te_6Pb)$]

Keithconnite-type telluride and plumbotelluride phases in the Kirakkajuppura deposit have the $Pd_{20}(Te,Pb)_7$ stoichiometry (Table 10). They occur as: (1) minute grains (≤10 μm in longest dimension: anal. 1 and 2) associated with chain-like micro-aggregates and enclosed within hydrous silicates, (2) a 50-μm grain (anal. 3) in intergrowth with vysotskite–braggite, and (3) a 20-μm grain (anal. 4, Table 10), located near the boundary of a subhedral grain of fine-grained Pd–Pb oxide, mantled by zvyagintsevite. The $Pd_{20}(Te,Pb)_7$-type phase (Table 10) seems to be related to the $Pd_{20}(Te,Se)_7$-type selenotelluride [$(Pd_{19.9}Pt_{0.07}Cu_{0.02}Fe_{0.02})_{\Sigma 20.01}(Te_{6.81}Se_{0.15}S_{0.03})_{\Sigma 6.99}$], reported from the Freetown layered complex, Sierra Leone (Bowles 2000). In addition, the present keithconnite-type phases are somewhat different from $Pd_{3-x}Te$ with $0.14 < x < 0.43$ for type keithconnite from the Stillwater complex, and keithconnite-like "$Pd_{19}(Te,Bi,Pb)_7$" phases, $Pd_{18.8–19.1}(Te,Pb,Bi)_{7.0}$ with 0.14–0.22 Pb *apfu* and 0.08–0.14 Bi *apfu*, in Cabri (1981). It should be noted that the type keithconnite differs slightly from synthetic $Pd_{20}Te_7$ (also reported as "Pd_3Te") in its X-ray powder-diffraction pattern; nevertheless, these natural and synthetic Pd tellurides are similar in crystal structure and cell size (Cabri *et al*. 1979).

The compositions (Table 10) indicate that 1 Pb *apfu* enters the $Pd_{20}(Te,Pb)_7$ solid solution, substituting for Te. Thus, our results appear to be consistent with a limited miscibility between keithconnite (trigonal $Pd_{3-x}Te$ or $Pd_{20}Te_7$) and zvyagintsevite (cubic Pd_3Pb; Cu_3Au structure-type). According to experimental data

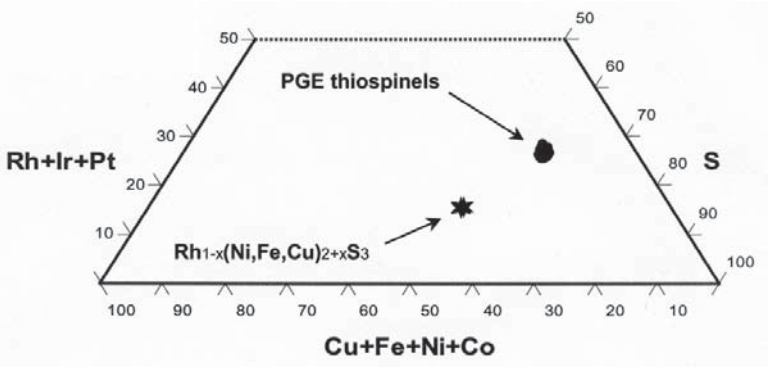

FIG. 14. Atom proportions of unnamed $Rh_{1-x}(Ni,Fe,Cu)_{2+x}S_3$ (n = 3: filled stars) and various PGE thiospinels of the cuprorhodsite – (ferrorhodsite) – cuproiridsite – malanite series (n = 424: circles) from the Kirakkajuppura deposit, Penikat complex, in terms of (Cu + Fe + Ni + Co) – (Rh + Ir + Pt) – S composition space.

(El-Boragy & Schubert 1971, Berlincourt *et al*. 1981), at 480°C, up to 0.27 Te *apfu* substitutes for Pb in a zvyagintsevite-type solid-solution: $Pd_3(Pb_{1-x}Te_x)$, and about the same maximum content of Pb (up to 0.26 *apfu*) can enter a synthetic keithconnite-type solid-solution: "$Pd_3(Te_{1-x}Pb_x)$".

Unnamed $Pd_5(As,Te,Sn,Pb)_2$

A complex plumbostannotelluro-arsenide of Pd is intimately associated with the Kuprikka mineralization, which forms part of the Kirakkajuppura PGE deposit, and occurs in the middle portion of a mineralized layer of peridotite cumulate. Results of a SEM–EDS analysis of this unusual phase gave: Pd 74.01, As 11.62, Te 9.20, Sn 4.98, and Pb 1.93, total 101.74 wt.%. The formula is $[Pd_{5.00}(As_{1.11}Te_{0.52}Sn_{0.30}Pb_{0.07})_{\Sigma 2.00}]$, which is remarkably stoichiometric, and suggests a relationship with synthetic $Pd_5(As_{2-x}Te_x)$, $0 \le x \le 1$, which is hexagonal and Pd_5As_2-type (El-Boragy & Schubert 1971, Berlincourt *et al*. 1981). Thus, about 0.5 Te *apfu*, 0.3 Sn *apfu* and 0.1 Pb *apfu* replace As in the phase from Kirakkajuppura; the observed (Te + Sn + Pb) value is thus about 0.9 *apfu*, which is close to the upper-limit value of 1 *apfu* reported for Te in synthetic $Pd_5(As_{2-x}Te_x)$. Presumably, larger amounts of Pb and greater variations among As, Te, Sn, and Pb may be observed in Pd_5As_2-related phases of this type. In addition, some other Pd arsenides are somewhat similar in composition to the $Pd_5(As,Te,Sn,Pb)_2$ phase from Kirakkajuppura: stillwaterite, hexagonal Pd_8As_3 (Cabri *et al*. 1975), arsenopalladinite, triclinic $Pd_8(As,Sb)_3$ (Cabri *et al*. 1977), and an unnamed orthorhombic Pd_5As_2 phase (Cabri *et al*. 1975). However, the Te-rich composition and the A_5B_2 (rather than A_8B_3) stoichiometry observed for the phase from Kirakkajuppura argue for a close relationship with synthetic $Pd_5(As_{2-x}Te_x)$ of El-Boragy & Schubert (1971).

TABLE 10. COMPOSITIONS OF KEITHCONNITE AND PLUMBIAN KEITHCONNITE FROM THE KIRAKKAJUPPURA PGE DEPOSIT

	Pd	Pt	Te	Bi	Pb	Total
1 wt.%	68.75	0.45	26.68	2.31	n.d.	98.19
2	68.48	0.83	26.19	2.35	n.d.	97.85
3	69.49	0.53	26.25	2.30	n.d.	98.57
4	68.69	n.d.	24.56	n.d.	6.75	100.0

	Pd	Pt	ΣPd, Pt	Te	Bi	Pb	ΣTe,Bi,Pb
1 *apfu*	20.08	0.07	20.15	6.50	0.34	-	6.84
2	20.10	0.13	20.23	6.41	0.35	-	6.76
3	20.20	0.08	20.28	6.37	0.34	-	6.71
4	20.02	-	20.02	5.97	-	1.01	6.97

Results of quantitative energy-dispersion analyses (SEM–EDS). The compositions are first expressed in wt.%. n.d.: not detected (<0.2-0.3 wt.%). 1, 2. Minute grains from chain-like micro-aggregates, enclosed within hydrous silicates. 3. About 50-μm grain intergrown with vysotskite-braggite. 4. A rim-like zone associated with a fine-grained Pd–Pb oxide grain. The atom proportions are based on a total of 27 atoms per formula unit (*apfu*).

Cu-rich, Pd-rich gold

A gold-rich alloy, corresponding to Cu-rich, Pd-rich gold $[Au_{76.1-81.1}Pd_{13.7-16.0}Cu_{6.1-6.3}Ag_{1.2-3.4}]$, is an important Pd-bearing phase in the Kirakkajuppura deposit. Several grains of the Au–Pd–Cu alloy, analyzed in this study, occur as inclusions in PGM (≤30 μm), or as large irregular grains; they all contain uniform levels of Pd: 8.5–9.4 wt.% (Table 11), which is distributed fairly homogeneously. The largest of these Au–Pd–Cu alloy grains (250 μm: Fig. 11C) is partially mantled by vysotskite $[Pd_{0.81-0.82}Pt_{0.15}Ni_{0.05}S_{0.98}]$, formed after the alloy grain.

Elevated contents of Pd in Au-rich alloys (Cu is not reported) are known in other layered complexes: Stillwater (6.6–7.3 wt.%) and Lac des Iles, Ontario, Canada (2.8–4.1 wt.% Pd: Cabri & Laflamme 1974, 1981). A relative enrichment in Cu (2.2 wt.%, or 6.1–6.6 at.% Cu: Table 11) is characteristic of the Au–Pd alloy from Kirakkajuppura. Pd-rich gold was also reported from the Cauê iron mine, Minas Gerais, Brazil (Olivo *et al*. 1994).

Relative abundances of the PGM

The modal proportions of the PGM at Kirakkajuppura are variable for *in situ* grains and heavy-mineral concentrates. In addition, the PGM are erratically distributed, which is typical of other PGE deposits associated with layered intrusions. Nevertheless, the relative abundances of the principal PGM species can be estimated. Our observations suggest that members of the vysotskite–braggite series (principally vysotskite, Pd-dominant) are generally preponderant in this deposit (*ca*. 40–45% of the PGM grains), followed by zvya-

TABLE 11. COMPOSITIONS OF Cu-RICH and Pd-RICH GOLD FROM THE KIRAKKAJUPPURA PGE DEPOSIT, PENIKAT COMPLEX, FINLAND

			Au	Pd	Cu	Ag	Total
EDS	1	wt.%	88.80	9.44	n.a.	1.77	100.0
EDS	2		87.14	8.83	2.26	1.98	100.2
EDS	3		88.22	8.52	2.33	2.03	101.1
EDS	4		86.77	8.86	2.23	2.14	100.0
WDS	5		87.54	8.72	2.24	0.74	99.24
	1	atom %	81.10	15.95	–	2.95	100
	2		76.37	14.32	6.14	3.17	100
	3		76.77	13.72	6.28	3.23	100
	4		76.13	14.38	6.06	3.43	100
	5		78.18	14.41	6.20	1.21	100

EDS: results of quantitative energy-dispersion analyses (SEM–EDS). WDS: result of wavelength-dispersion electron-microprobe analysis. Pt, Rh, Fe, and Ni were not detected; n.a.: not analyzed.

gintsevite (*ca*. 20–25%), unnamed Pd–Pb oxide (*ca*. 15–20%), PGE thiospinels of the cuprorhodsite–(ferrorhodsite)–malanite series (*ca*. 10–15%), laflammeite (up to 5%), and laurite–erlichmanite (up to 5%).

Zn-rich copper (*artificial or natural?*)

A round grain of Cu–Zn alloy (about 80 μm in diameter) was observed in a heavy-mineral concentrate sample from the Kirakkajuppura deposit. Its composition (SEM–EDS) is Cu 90.04 and Zn 9.37, total 99.41 wt.%, corresponding to [$Cu_{90.82}Zn_{9.18}$: at.%]. Native copper was also observed in this sample. The origin of this Zn-rich alloy, which may be an artifact, is uncertain. On the other hand, the presence of Cu-rich intermetallic compounds and alloys at Kirakkajuppura, such as skaergaardite [(Pd,Pt)Cu] and Pd–Pt–Cu alloy, implies a possible natural origin for the Zn-rich copper. A natural origin is also supported by occurrences of similar material at other localities, *e.g.*, a Mid-Atlantic Ridge hydrothermal deposit (Mozgova *et al*. 1996).

Unnamed $Pb_4O(VO_4)_2$

An unnamed Pb–V oxide [“$Pb^{2+}{}_4V^{5+}{}_2O_9$”] occurs as a cleavage filling in actinolite, similar to an occurrence of a microcrystalline aggregate of zvyagintsevite (Barkov *et al*. 1999a). The revised formula of $Pb_4O(VO_4)_2$ is based on the structural study of Krivovichev & Burns (2003).

Undefined Pb-rich iron silicate (*hydrous?*)

This phase occurs as a small, elongate grain (*ca*. 50 × 10 μm) enclosed within an anhedral grain of vysotskite. The EMP analysis gave: PbO 23.32, FeO 42.73, CaO 0.30, SiO_2 12.35, and Al_2O_3 0.98; the observed total is low (*ca*. 80%), implying the possible presence of OH or H_2O.

Unnamed (Th,Ca)(V^{5+},Si,P)O_4, and associated zircon, baddeleyite, barite, and a phosphatian huttonite or thorite [(Th,Fe,Ca)($Si_{0.7}P_{0.3}$)O_4] from a gabbro-pegmatite in the Kirakkajuppura area

A new Th-rich phase occurs at Kirakkajuppura as a tiny grain (12 × 5 μm), enclosed in a secondary silicate, in a pegmatitic gabbro (sample 433–PTPRO), hosted by a plagioclase–clinopyroxene–(augite)–orthopyroxene adcumulate of the MCU III. The phase is of complex composition: ThO_2 61.3, SiO_2 6.4, V_2O_5 17.5, P_2O_5 5.4, CeO_2 1.7, PbO 2.5, CaO 5.3, FeO 2.3, and total 102.4 wt.% (SEM–EDS). The formula, calculated on the basis of four oxygen atoms, is stoichiometric: $(Th_{0.62}Ca_{0.25}Fe_{0.08}Pb_{0.03}Ce_{0.03})_{\Sigma 1.01}(V^{5+}{}_{0.51}Si_{0.28}P_{0.20})_{\Sigma 0.99}O_4$, and the general formula is (Th,Ca)(V^{5+},Si,P)O_4. We are not aware of the existence of a mineral species of this composition. The alternative formulae, (Th,Ca)$V^{5+}{}_{0.5}$(Si,P)$_{0.5}O_4$ or (Th,Ca)$_2V^{5+}$(Si,P)O_8, appear less probable. This phosphosilicovanadate may represent a new (V-dominant) member of the monazite group, related to huttonite [monoclinic $ThSiO_4$] and brabantite [$Ca_{0.5}Th_{0.5}(PO_4)$], or, alternatively, to thorite [tetragonal $ThSiO_4$]. Unfortunately, the minute grain-size of this phase precludes a more detailed examination.

Other uncommon accessories, identified as minute grains in this sample of pegmatitic gabbro, are: *barite* of composition BaO 64.3, SrO 1.3, SO_3 34.4, for a total of 100.0 wt.% (SEM–EDS), formula $(Ba_{0.98}Sr_{0.03})_{\Sigma 1.01}(SO_4)$, *zircon*, a Hf-bearing *baddeleyite* [$(Zr_{0.99}Hf_{0.01})O_2$], and yet another Th-based phase (10 × 10 μm): (Th,Fe,Ca)($Si_{0.7}P_{0.3}$)O_4, probably corresponding to *phosphatian huttonite* or *phosphatian thorite*.

Discussion, Implications, and Conclusions

Noble-metal geochemistry, and comparison with other PGE deposits associated with layered intrusions

Several important features, presented in Figure 15, distinguish the Kirakkajuppura PGE deposit from the other PGE deposits associated with layered complexes. These features include: (1) anomalously high contents of Pd + Pt (Fig. 15A), observed locally, which exceed values reported for the world-class PGE deposits in the literature (*cf*. Barnes & Naldrett 1985, McDonald & Vaughan 1995, Barnes & Maier 2002). (2) Anomalously low S contents in PGE-rich samples, and the absence of statistically significant correlations between the PGE and S; in contrast, note that a positive PGE + Au *versus* S correlation (Fig. 15B) is evident for the J–M reef samples (Barnes & Naldrett 1985). On the contrary, the highest PGE contents are observed in S-poor samples from Kirakkajuppura, so that the PGE + Au *versus* S correlation tends to be slightly negative (Fig. 15B). This observation is corroborated by our mineralogical data, indicating that the coarse-grained aggregates of PGM (*e.g.*, Fig. 3) are not associated with base-metal sulfides, which are present only in trace or minor quantities in the mineralized rocks. Also, note that the PGE + Au values do not correlate with Cr contents (Fig. 15C), and no correlation is observed between modal amounts of PGM and chromite. In addition, there is no relationship between whole-rock levels of MgO and PGE + Au; thus, the PGE-rich mineralization at Kirakkajuppura is not controlled by a specific type of cumulate, and is associated with various mafic to ultramafic rocks (Fig. 15D). (3) The anomalously PGE-rich rocks from Kirakkajuppura, which are strongly “depleted” in S (Fig. 15B), are also poor in overall Cu and Ni (Figs. 15E, F), again consistent with the extreme scarcity of base-metal sulfides in the PGE-rich rocks. The PGE-rich rocks from other “low-sulfide” deposits, associated with the Bushveld and Stillwater complexes, are notably richer in Cu and Ni (Figs. 15E, F).

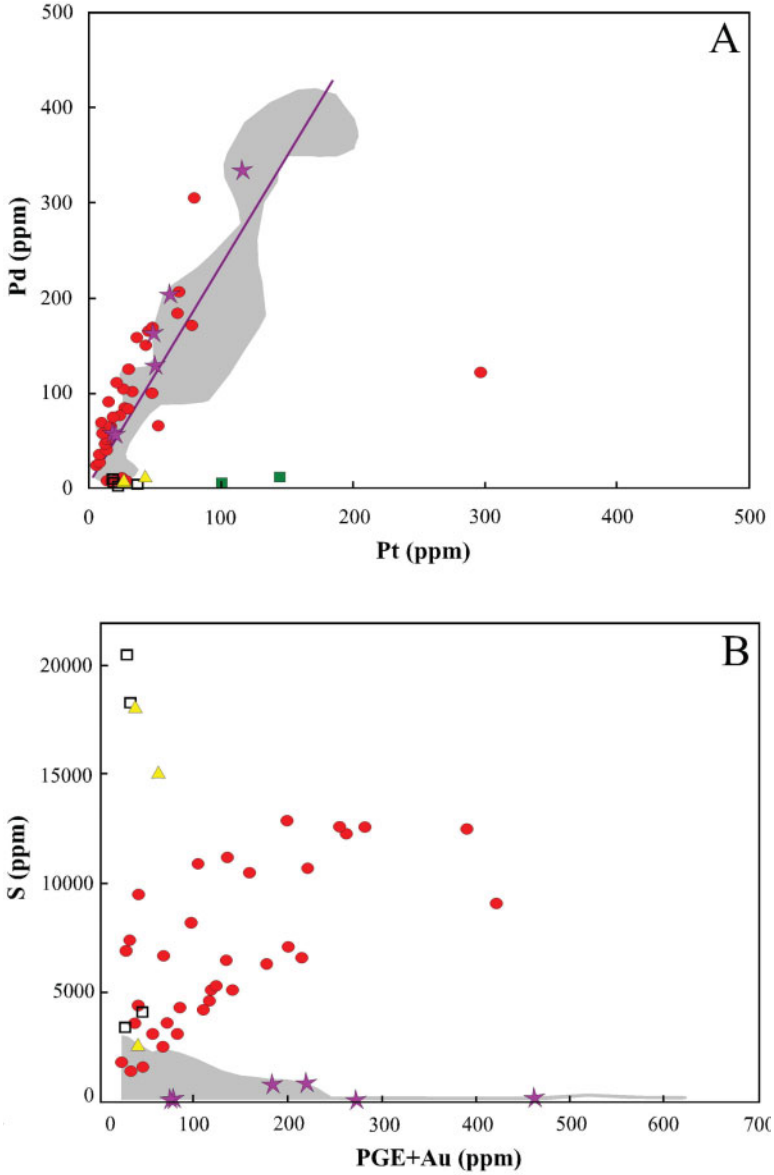

FIG. 15. Binary plots: Pt *versus* Pd (A), PGE + Au *versus* S (B), PGE + Au *versus* Cr (C), PGE + Au *versus* MgO (D), PGE + Au *versus* Cu (E), and PGE + Au *versus* Ni (F) for selected PGE-rich rocks from the Kirakkajuppura deposit, Penikat layered complex, Finland. The filled stars are the whole-rock data, published for the Kirakkajuppura deposit in Halkoaho *et al*. (1989) and Barkov *et al*. (1999a). The shaded area displays the overall whole-rock variations, observed for the Kirakkajuppura deposit on the basis of a total of 152 samples (unpubl. data of Halkoaho *et al*.), containing at least 20 ppm (PGE + Au), where the PGE are (Pd + Pt + Rh) expressed in ppm. For comparison, published whole-rock data on selected PGE-rich samples are also plotted, representing the J–M reef, Stillwater layered complex (Barnes & Naldrett 1985: filled circles), the Merensky reef, Bushveld layered complex (Barnes & Maier 2002: open squares), the mineralized boulder bed, Rustenburg layered suite, Bushveld complex (Maier & Barnes 2003: triangles), and platiniferous dunite pipes, Bushveld complex (McDonald & Vaughan 1995: filled squares).

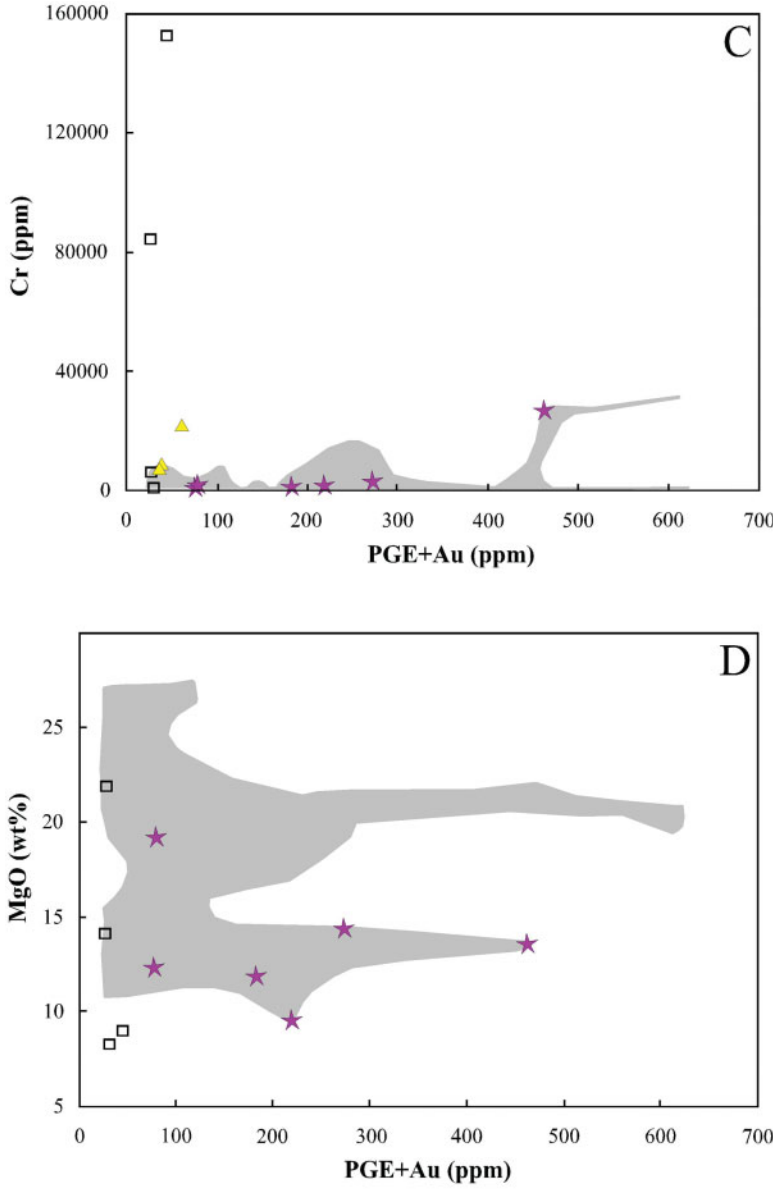

Barkov *et al*. (1999a) noted that some whole-rock compositions, representative of the Kirakkajuppura deposit, are strongly enriched in Pd + Pt and extremely poor in S, and display values of their atomic (Pd + Pt): S ratio of approximately 1:1, corresponding to vysotskite–braggite. For example, the following whole-rock contents: Pd 203, Pt 60.6, and S 70 ppm, recalculated on the basis of Σatoms = 2, give vysotskite-type proportions: $(Pd_{0.87}Pt_{0.14})_{\Sigma 1.01}S_{0.99}$. This observation is consistent with the abundance of vysotskite–braggite at Kirakkajuppura, which is typically Pd-dominant and poor in Ni [*e.g.*, the mean composition is $(Pd_{0.74}Pt_{0.23}Ni_{0.05})_{\Sigma 1.02}S_{0.99}$, for $n = 60$ in this study]. On the other hand, our observations, based on a total of 152 rock samples from Kirakkajuppura (Halkoaho 1993, Barkov *et al*. 1999a, Halkoaho *et al*., unpubl. data), containing at least 20 ppm (Pd,Pt,Rh) + Au each, indicate that the Pd *versus* Pt correlation is strongly positive, with a correlation coefficient of 0.96 and a mean Pd:Pt ratio of 2.44 (Fig. 15A). The existence of this positive

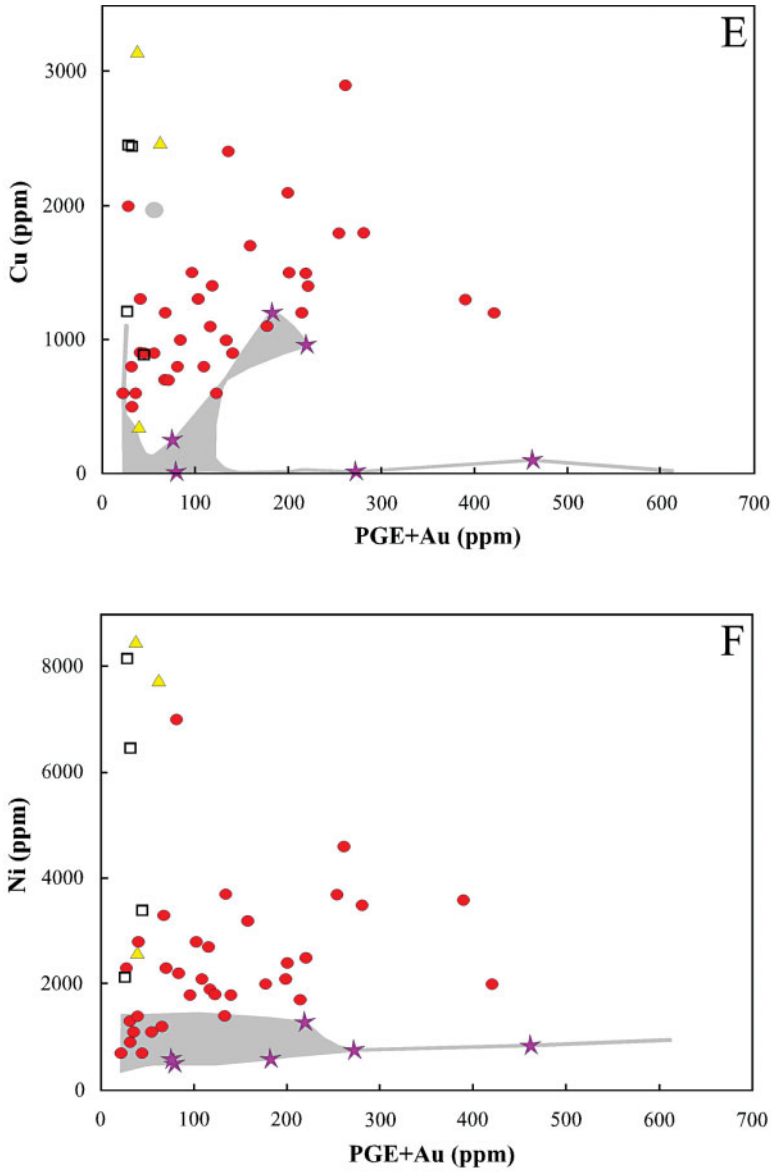

correlation cannot be accounted for by modal variations in the vysotskite–braggite alone. On the contrary, such variations would have resulted in a negative Pd *versus* Pt correlation, because of the Pd-for-Pt substitution in the vysotskite–braggite series (Fig. 4). This series only exhibits an essential Pd-for-Pt substitution, whereas other PGM observed at Kirakkajuppura are rich in either Pd or Pt. Thus, the observed sympathetic relationship between Pd and Pt (Fig. 15A) must be related to modal variations in amounts of various coexisting Pd- and Pt-based species in the PGE-mineralized rocks.

The covariation of the associated Pd and Pt (Fig. 15A), which are the principal PGE in this deposit, may reflect a preferential mobility of Pd and Pt, compared to the other PGE, in a hydrothermal system. The mean value of the ratio Pd:Pt is about 2, which suggests that Pd was preferentially remobilized (relative to Pt) and transported by a mobile fluid. In general, varying values of the Pd:Pt ratio and of other similar ratios, observed for mineralized rocks in hydrothermal PGE deposits, may be a reflection of fluid composition and physicochemical conditions of crystallization,

which control a fluid's capability to remobilize and transport various proportions of the PGE.

Other important characteristics of the PGE mineralization at Kirakkajuppura, extremely low levels of S in the system, and their mineralogical consequences

Anomalously low overall S contents are characteristic of the PGE-mineralized rocks in the Kirakkajuppura deposit (Fig. 15B). Owing to the extremely S-poor environment, some unusual PGM species crystallized in this deposit. These are uncharacteristic of layered intrusions, and are rather typical of low-S deposits associated with various Uralian–Alaskan-type (zoned) and ophiolite complexes. These unusual PGM, observed at Kirakkajuppura, are various PGE-rich thiospinels [cuprorhodsite–(ferrorhodsite)–cuproiridsite–malanite series], konderite-like Pb–(Pd)-rich sulfides, including a Fe-dominant analogue of konderite, and unnamed $Rh_{1-x}(Ni,Fe,Cu)_{2+x}S_3$. The occurrence of laflammeite [$Pd_3Pb_2S_2$], having a high ΣMe:S ratio of 2.5, is also a result of the S-depleted environment. Rhodplumsite [$Rh_3Pb_2S_2$], having similar atomic proportions, was reported only from a placer derived from a Uralian-type complex (Genkin *et al*. 1983).

Textural evidence (Fig. 11D) suggests that unnamed $Rh_{1-x}(Ni,Fe,Cu)_{2+x}S_3$ formed by the replacement of coexisting millerite. We hypothesize that with progressive crystallization of millerite, the residual fluid or liquid became saturated in the incompatible elements: Rh, Fe, and Cu. Schematically, this reaction may be represented as: [NiS] *millerite* + [Rh + (Fe,Cu) + S_2] *fluid* = unnamed [$Rh(Ni,Fe,Cu)_2S_3$].

Note that the abundance of various S-bearing PGM species in the Kirakkajuppura deposit contrasts with the low bulk contents of S, observed in PGE-rich rocks from this deposit. This feature is similar to that reported from chromitite layers in layered intrusions (Barkov & Fleet 2004, and references therein), where a subsolidus re-equilibration between chromite and sulfide is believed to have caused loss of Fe from the sulfide and relative enrichment in S (Cu, and Ni) in the associated sulfide assemblages (Von Gruenewaldt *et al*. 1986). The following observations also support the existence of a certain similarity between the Kirakkajuppura deposit and PGE-mineralized chromitites in layered intrusions: (1) only trace or minor amounts of base-metal sulfides are observed; (2) the base-metal sulfide minerals are characteristically enriched in Cu or Ni and relatively poor in Fe (Table 3); (3) laurite–erlichmanite, which is intimately associated with chromitites in other localities, is relatively abundant in association with the hydrous silicates in the Kirakkajuppura deposit. It is noteworthy that a hydrothermal origin of laurite–erlichmanite is possible (Barkov & Fleet 2004). On the other hand, the PGE mineralization from Kirakkajuppura displays important differences from PGE mineralized chromitites, such as the Pd-dominant character, and, locally, very high PGE contents, which are about two orders of magnitude higher than those typical of mineralized chromitites in layered intrusions. Also, the observed grain-size of euhedral laurite–erlichmanite at Kirakkajuppura is anomalously large (up to 0.3 mm), contrasting with minute laurite–erlichmanite grains (up to 20 μm) from chromitite layers of layered intrusions.

It is known that the PGE are strongly partitioned into segregating sulfide liquid, consistent with high values of partition coefficients of the PGE between sulfide and basaltic liquid (Fleet *et al*. 1996). However, the PGE-rich mineralization at Kirakkajuppura, which is extremely poor in S, could not have formed *in situ* as a result of the collection of PGE by a magmatic sulfide liquid. The intimate association with the hydrous silicates, and the observed veinlet- and chain-like morphology of various PGM aggregates (*e.g*., Figs. 3, 7C, and Barkov *et al*. 1999a) is consistent with a postmagmatic–hydrothermal deposition of the PGM.

Abundance of Pb-rich PGM, and oxidizing conditions of crystallization

The observed Pb enrichment is characteristic of many PGM and associated minerals in the Kirakkajuppura deposit: zvyagintsevite, unnamed Pd_7PbO_8, laflammeite, konderite-like Pb–(Pd)-rich sulfides, $Pd_5(As,Te,Sn,Pb)_2$, $Pd_{20}(Te,Pb)_7$, $Pb_4O(VO_4)_2$, and the undefined Pb-rich hydrous silicate. In contrast, Pb-bearing PGM are very rare species in other PGE deposits associated with layered intrusions.

Strongly oxidizing conditions appear to have prevailed at advanced and late stages of postmagmatic–hydrothermal crystallization, when various "mega"- and "micro"-aggregates of PGM were presumably deposited at Kirakkajuppura. Evidence for an oxidizing environment of PGM crystallization includes: (1) abundant grains of Pd_7PbO_8 oxide phase, which displays complementary textural relationships with the associated end-member zvyagintsevite (Pd_3Pb). Thus, we suggest that the zvyagintsevite likely interacted with a late highly oxidizing fluid, and, consequently, was converted to the Pd–Pb oxide, *via* the following oxidation reaction: $7Pd_3Pb + 14O_2 = 3Pd_7PbO_8 + 4PbO$. The "4PbO" amount, produced by this reaction could be incorporated in the $Pb_4O(VO_4)_2$ oxide phase *via* a reaction of the type: $4PbO + V_2O_5$ (*fluid*) = $Pb_4O(VO_4)_2$, or in the observed Pb-rich hydrous(?) silicate, for example.

This occurrence of the Pd-rich oxysalt mineral is highly unusual, although not unique, for a PGE deposit associated with a layered intrusion. Various Pd–Sb–Bi oxide phases have been reported from "exocontact" sulfide ores, which are in contact with host sandstones, in the Chiney layered anorthosite–gabbronorite complex, Aldan shield, Russia (Tolstykh *et al*. 2000). Note that the Kirakkajuppura deposit is also located near the end of the layered complex and relatively

adjacent to wallrocks (Fig. 1), so that influx of external oxidizing fluids could be possible for the PGE deposits associated with the Penikat and Chiney complexes. In addition, highly oxidizing conditions of crystallization are also characteristic of unusual Pt–Pd mineralization, hosted by quartz veins, associated with the Bushveld complex, although no PGE-rich oxides were observed in these veins (McDonald & Vaughan 1995).

The following observations also argue for an oxidation regime at late stages of crystallization in the Kirakkajuppura area of the Penikat complex: (1) the inferred valence state of V is 5+ in unnamed $Pb_4O(VO_4)_2$, associated with the zvyagintsevite micro-aggregate, and in unnamed $(Th,Ca)(V^{5+},Si,P)O_4$ from a pegmatitic gabbro in this area. It is known that V is a sensitive indicator of volatile-rich environments, existing at postcumulus stages of crystallization of mafic–ultramafic complexes. The observed occurrence of manganoan ilmenite (up to 11 wt.% MnO: Table 2) is also consistent with a postmagmatic environment rich in volatile components; and (2) the inferred valence state of Fe is ferric in the PGE thiospinels, which are common at Kirakkajuppura and enriched in the ferrorhodsite end-member $[(Fe^{3+}_{0.5}Cu^{+}_{0.5})Rh^{3+}_2S^{2-}_4]$.

Concluding remarks

The megacyclic units I to III of the Penikat complex likely crystallized from a boninitic parental magma (Alapieti & Halkoaho 1995, and references therein), which could be undersaturated in S and relatively enriched in PGE, Pb, H_2O, and other volatile species and incompatible elements (note, for example, the reported occurrence of Th-rich phases in the pegmatitic gabbro at Kirakkajuppura). The Kirakkajuppura PGE deposit was likely formed as a result of efficient hydrothermal remobilization and transport of PGE from their initial sites of deposition, probably associated with "primary" Pd–Pt zones of the low-sulfide SJ reef and also with some Ru–Os-mineralized chromitite zones, toward the northern end of the Penikat complex. This hydrothermal process probably led to the local deposition of the "bonanza"-type Kirakkajupura PGE mineralization in intimate association with the hydrous silicate minerals.

Acknowledgements

This study was supported by the Natural Sciences and Engineering Research Council of Canada. Thanks are due to the organizing committee of the IGCP Project 336 Symposium in Rovaniemi (1996, Finland) for its assistance in collecting samples from the Kirakkajuppura PGE deposit. A.Y.B. is grateful to the late A.J. Criddle, A.C. Roberts, Y.A. Pakhomovsky, Y.P. Men'shikov, G. Poirier, R. Peura, and O. Taikina-aho for their various and helpful assistance at various stages of this study. We thank J.H.G. Laflamme, K. Kojonen, and guest Associate Editor Yuanming Pan for helpful comments on this contribution. The breadth of Michael Fleet's involvement in the Earth Sciences is awesome. It encompasses the pattern of behavior of the platinum-group elements in magmatic and hydrothermal systems. The first, third and fourth authors are thrilled to dedicate this contribution to him on this occasion.

References

Ahmed, A.H. & Arai, S. (2003): Platinum-group minerals in podiform chromitites of the Oman ophiolite. *Can. Mineral.* **41**, 597-616.

Alapieti, T.T. & Halkoaho, T.A.A. (1995): Cryptic variation of augite in the Penikat layered intrusion, northern Finland, with reference to megacyclic units and PGE-enriched zones. *Mineral. Petrol.* **54**, 11-24.

_____ & Lahtinen, J.J. (1986): Stratigraphy, petrology, and platinum group element mineralization of the Early Proterozoic Penikat layered intrusion, northern Finland. *Econ. Geol.* **81**, 1126-1136.

_____ & _____ (1989): Penikat Intrusion. *In* Early Proterozoic Layered Intrusions in the Northeastern Part of the Fennoscandian Shield (T. Alapieti, ed.). *Fifth Int. Platinum Symp., Guide to the Post-Symposium Field Trip, Geol. Surv. Finland, Guide* **29**, 15-21.

Barkov, A.Y. & Fleet, M.E. (2004): An unusual association of hydrothermal platinum-group minerals from the Imandra layered complex, Kola Peninsula, northwestern Russia. *Can. Mineral.* **42**, 455-467.

_____, _____, Martin, R.F. & Alapieti, T.T. (2004a): Zoned sulfides and sulfarsenides of the platinum-group elements from the Penikat layered complex, Finland. *Can. Mineral.* **42**, 515-537.

_____, _____, _____ & Halkoaho, T.A.A. (2004b): A potentially new konderite-like sulfide of Fe, Pb, Cu, Rh, Pd, and Ir from the Penikat layered complex, Finland. *Can. Mineral.* **42**, 499-513.

_____, Halkoaho, T.A.A., Roberts, A.C., Criddle, A.J., Martin, R.F. & Papunen, H. (1999a): New Pd-Pb and Pb-V oxides from a bonanza-type PGE-rich, nearly BMS-free deposit in the Penikat layered complex, Finland. *Can. Mineral.* **37**, 1507-1524.

_____, Martin, R.F., Halkoaho, T.A.A. & Criddle, A.J. (2002): Laflammeite, $Pd_3Pb_2S_2$, a new platinum-group mineral species from the Penikat layered complex, Finland. *Can. Mineral.* **40**, 671-678.

_____, _____, _____ & Poirier, G. (2000): The mechanism of charge compensation in Cu-Fe-PGE thiospinels from the Penikat layered intrusion, Finland. *Am. Mineral.* **85**, 694-697.

_____, Pakhomovskii, Y.A. & Men'shikov, Y.P. (1995): Zoning in the platinum-group sulfide minerals from the

Lukkulaisvaara and Imandrovsky layered intrusions, Russia. *Neues Jahrb. Mineral., Abh.* **169**, 97-117.

_____, THIBAULT, Y., LAAJOKI, K.V.O, MELEZHIK, V.A. & NILSSON, L.P. (1999b): Zoning and substitutions in Co–Ni–(Fe)–PGE sulfarsenides from the Mount General'skaya layered intrusion, Arctic Russia. *Can. Mineral.* **37**, 127-142.

BARNES, S.-J. & MAIER, W.D. (2002): Platinum-group elements and microstructures of normal Merensky Reef from Impala platinum mines, Bushveld complex. *J. Petrol.* **43**, 103-128.

BARNES, S.J. & NALDRETT, A.J. (1985): Geochemistry of the J–M (Howland) Reef of the Stillwater complex, Minneapolis Adit area. I. Sulfide chemistry and sulfide–olivine equilibrium. *Econ. Geol.* **80**, 627-645.

BERLINCOURT, L.E., HUMMEL, H.H. & SKINNER, B.J. (1981): Phases and phase relations of the platinum-group elements. *In* Platinum-Group Elements: Mineralogy, Geology, Recovery (L.J. Cabri, ed.). *Can. Inst. Mining Metall., Spec. Vol.* **23**, 19-45.

BETTAHAR, N., CONFLANT, P. & ABRAHAM, F. (1992): Effect of copper substitution on the electrical transport properties of $(Bi,Pb)_2MO_4$ (M = Pd, Pt) linear chain compounds. *J. Alloys Compd.* **188**, 211-214.

BOWLES, J.F.W. (2000): Prassoite, vysotskite and keithconnite from the Freetown layered complex, Sierra Leone. *Mineral. Petrol.* **68**, 75-84.

CABRI, L.J. (1981): The platinum-group minerals. *In* Platinum-Group Elements: Mineralogy, Geology, Recovery (L.J. Cabri, ed.). *Can. Inst. Mining Metall., Spec. Vol.* **23**, 83-150.

_____, CLARK, A.M. & CHEN, T.T. (1977): Arsenopalladinite from Itabira, Brazil, and from the Stillwater Complex, Montana. *Can. Mineral.* **15**, 70-73.

_____, HARRIS, D.C. & WEISER, T.W. (1996): Mineralogy and distribution of platinum-group mineral (PGM) placer deposits of the world. *Explor. Mining Geol.* **5**, 73-167.

_____ & LAFLAMME, J.H.G. (1974): Rhodium, platinum, and gold alloys from the Stillwater Complex. *Can. Mineral.* **12**, 399-403.

_____ & _____ (1981): Analyses of minerals containing platinum-group elements. *In* Platinum-Group Elements: Mineralogy, Geology, Recovery (L.J. Cabri, ed.). *Can. Inst. Mining Metall., Spec. Vol.* **23**, 151-173.

_____, _____, STEWART, J.M., ROWLAND, J.F. & CHEN, T.T. (1975): New data on some palladium arsenides and antimonides. *Can. Mineral.* **13**, 321-335.

_____, _____, _____, TURNER, K. & SKINNER, B.J. (1978): On cooperite, braggite, and vysotskite. *Am. Mineral.* **63**, 832-839.

_____, ROWLAND, J.F., LAFLAMME, J.H.G. & STEWART, J.M. (1979): Keithconnite, telluropalladinite and other palladium–platinum tellurides from the Stillwater Complex, Montana. *Can. Mineral.* **17**, 589-594.

_____ & TRAILL, R.J. (1966): New palladium minerals from Noril'sk, western Siberia. *Can. Mineral.* **8**, 541-550.

DUBLER, E., VEDANI, A. & OSWALD, H.R. (1983): New structure determination of murdochite, Cu_6PbO_8. *Acta Crystallogr.* **C39**, 1143-1146.

EL-BORAGY, M. & SCHUBERT, K. (1971): On a variety of NiAs-family compounds of palladium with *B* elements. *Z. Metallkunde* **62**, 314-323.

FLEET, M.E., CROCKET, J.H. & STONE, W.E. (1996): Partitioning of platinum-group elements (Os, Ir, Ru, Pt, Pd) and gold between sulfide liquid and basalt melt. *Geochim. Cosmochim. Acta* **60**, 2397-2412.

_____, DE ALMEIDA, C.M. & ANGELI, N. (2002): Botryoidal platinum, palladium and potarite from the Bom Sucesso stream, Minas Gerais, Brazil: compositional zoning and origin. *Can. Mineral.* **40**, 341-355.

GARUTI, G., GAZZOTTI, M. & TORRES-RUIZ, J. (1995): Iridium, rhodium, and platinum sulfides in chromitites from the ultramafic massifs of Finero, Italy, and Ojen, Spain. *Can. Mineral.* **33**, 509-520.

GENKIN, A.D., MURAV'YEVA, I.V. & TRONEVA, N.V. (1966): Zvyagintsevite: natural intermetallic compound of Pd, Pt, Pb, and Sn. *Geol. Rudn. Mestorozhd.* **8**, 94-100 (in Russ.)

_____, VYAL'SOV, L.N., EVSTIGNEEVA, T.L., LAPUTINA, I.P. & BASOVA, G.V. (1983): Rhodplumsite $Rh_3Pb_2S_2$ – a new sulfide of rhodium and lead. *Mineral. Zh.* **5**(2), 87-91 (in Russ.).

HALKOAHO, T.A.A. (1993): The Sompujärvi and Ala-Penikka PGE reefs in the Penikat layered intrusion, northern Finland: implications for PGE reef-forming processes. *Acta Univ. Oul.* **A 249**, Univ. of Oulu, Oulu, Finland.

_____, ALAPIETI, T.T. & LAHTINEN, J.J. (1989a): The Sompujärvi PGE mineralization in the Penikat layered intrusion, Northern Finland. *In* Early Proterozoic layered intrusions in the northeastern part of the Fennoscandian Shield (T. Alapieti, ed.). *Fifth Int. Platinum Symp., Guide to the Post-Symposium Field Trip, Geol. Surv. Finland., Guide* **29**, 71-92.

_____, _____ & _____ (1989b): The Sompujärvi PGE mineralization in the Kirakkajuppura area. Descriptions of Post-Symposium Field Excursion Sites. Site 6. *In* Early Proterozoic Layered Intrusions in the Northeastern Part of the Fennoscandian Shield (T. Alapieti, ed.). *Fifth Int. Platinum Symp., Guide to the Post-Symposium Field Trip, Geol. Surv. Finland, Guide* **29**, 212-216.

_____, _____ & _____ (1990): The Sompujärvi PGE Reef in the Penikat layered intrusion, northern Finland. *Mineral. Petrol.* **42**, 39-55.

KNOP, O., HUANG, C.-H., REID, K.I.G. & CARLOW, J.S. (1976): Chalcogenides of the transition elements. X. X-ray, neutron, Mössbauer and magnetic studies of pentlandite and the π phases, π (Fe, Co, Ni, S), Co_8MS_8 and $Fe_4Ni_4MS_8$ (M = Ru, Rh, Pd). *J. Solid State Chem.* **16**, 97-116.

KRIVOVICHEV, S.V. & BURNS, P.C. (2003): Chains of edge-sharing OPb_4 tetrahedra in the structure of $Pb_4O(VO_4)_2$ and in related minerals and inorganic compounds. *Can. Mineral.* **41**, 951-958.

KWITKO, R., CABRAL, A.R., LEHMANN, B., LAFLAMME, J.H.G., CABRI, L.J., CRIDDLE, A.J. & GALBIATTI, H.F. (2002): Hongshiite, PtCu, from itabirite-hosted Au-Pd-Pt mineralization (jacutinga), Itabira district, Minas Gerais, Brazil. *Can. Mineral.* **40**, 711-723.

MAIER, W.D. & BARNES S.-J. (2003): Platinum-group elements in the Boulder Bed, western Bushveld Complex, South Africa. *Mineral. Deposita* **38**, 370-380.

MCDONALD, I. & VAUGHAN, D.J. (1995): Platinum mineralization in quartz veins near Naboomspruit, central Transvaal. *S. Afr. J. Geol.* **98**, 168-175.

MOZGOVA, N.N., KRASNOV, S.G., BATUYEV, B.N., BORODAEV, Y.S., EFIMOV, A.V., MARKOV, V.F. & STEPHANOVA, T.V. (1996): The first report of cobalt pentlandite from a Mid-Atlantic Ridge hydrothermal deposit. *Can. Mineral.* **34**, 23-28.

MULLER, O. & ROY, R. (1971): Synthesis and crystal chemistry of some new complex palladium oxides. *Advan. Chem. Ser.* **98**, 28-38.

OLIVO, G.R. & GAUTHIER, M. (1995): Palladium minerals from the Cauê iron mine, Itabira District, Minas Gerais, Brazil. *Mineral. Mag.* **59**, 455-463.

_____, _____ & BARDOUX, M. (1994): Palladian gold from the Cauê iron mine, Itabira district, Minas Gerais, Brazil. *Mineral. Mag.* **58**, 579-587.

RUDASHEVSKY, N.S., MCDONALD, A.M., CABRI, L.J., NIELSEN, T.F.D., STANLEY, C.J., KRETZER, YU.L. & RUDASHEVSKY, V.N. (2004): Skaergaardite, PdCu, a new platinum-group intermetallic mineral from the Skaergaard intrusion, Greenland. *Mineral. Mag.* **68**, 615-632.

_____, MOCHALOV, A.G., TRUBKIN, N.V., GORSHKOV, A.I., MEN'SHIKOV, Y.P. & SHUMSKAYA, N.I. (1984): Konderite $Cu_3Pb(Rh,Pt,Ir)_8S_{16}$ – a new mineral. *Zap. Vses. Mineral. Obshchest.* **113**, 703-712 (in Russ.).

SMALLWOOD, P.L., SMITH, M.D. & LOYE, H.-C. (2000): Flux synthesis of alkaline earth palladates. *J. Crystal Growth* **216**, 299-303.

TOLSTYKH, N.D., KRIVENKO, A.P., LAVRENT'EV, Y.G., TOLSTYKH, O.N. & KOROLYUK, V.N. (2000): Oxides of the Pd–Sb–Bi system from the Chiney massif, Aldan Shield, Russia. *Eur. J. Mineral.* **12**, 431-440.

TORRES-RUIZ, J., GARUTI, G., GAZZOTTI, M., GERVILLA, F. & HACH-ALÍ, P.F. (1996): Platinum-group minerals in chromitites from the Ojen lherzolite massif (Serrania de Ronda, Betic Cordillera, southern Spain). *Mineral. Petrol.* **56**, 25-50.

VERRYN, S.M.C. & MERKLE, R.K.W (2002): The system PtS–PdS–NiS between 1200° and 700°C. *Can. Mineral.* **40**, 571-584.

VON GRUENEWALDT, G., HATTON, C.J., MERKLE, R.K.W. & GAIN, S.B. (1986): Platinum-group element – chromitite associations in the Bushveld complex. *Econ. Geol.* **81**, 1067-1079.

WASEL-NIELEN, H.D. & HOPPE, R. (1970): Calcium oxide – palladium oxide and strontium oxide – palladium oxide systems. *Z. Anorg. Allg. Chem.* **375**, 209-213.

WASER, J. & MCCLANAHAN, E.D., JR. (1952): Structure of $Na_xPt_3O_4$. *J. Chem. Phys.* **20**, 199.

WINKLER, B., CHALL, M., PICKARD, C.J., MILMAN, V. & WHITE, J. (2000): Structure of Cu_6PbO_8**.** *Acta Crystallogr.* **B56**, 22-26.

Received February 9, 2005, revised manuscript accepted August 1, 2005.

APPENDIX: ANALYTICAL METHODS

Whole-rock analyses

Each representative sample was analyzed for nineteen elements by X-ray fluorescence (XRF) at the Research Laboratory of the Rautaruukki Oy Steel Works, Raahe, Finland, and at the Geo-analytical Laboratory of the Outokumpu Oy, Finland. Noble metal contents were determined from 50-g samples by INAA after preconcentration into a nickel sulfide bead at the Becquerel Laboratories, Toronto, Canada, and by a combined fire-assay and atomic absorption spectroscopy procedure at the Rautaruukki Oy Laboratory.

Electron-microprobe analyses, EMPA (WDS and SEM–EDS)

Electron-microprobe analyses of PGM were carried out by wavelength-dispersion spectrometry (WDS), using different instruments, analytical conditions, and sets of standards. A JEOL JXA–8900 electron microprobe was operated at 20 kV and 30 nA. A finely focused beam and the following X-ray lines and set of standards were used: Ru*L*α, Os*L*α, Ir*L*α, Rh*L*α, Pt*L*α, Pd*L*β (pure metals: Ru, Os, Ir, Rh, Pt, and Pd), Fe*K*α (FeS_2), Ni*K*α, Co*K*α (CoNiAs), Pb*M*α (PbS), S*K*α (PbS), and As*L*β ($PtAs_2$). The raw data were processed and corrected on-line using the ZAF (JEOL) and CTZ programs. A JEOL–733 electron microprobe was operated at 15 kV and 15 nA. The following X-ray lines and standards were used: Pd*L*α, Pt*L*α, Ir*L*α, Rh*L*α, Ru*L*α, Os*L*α, Ag*L*α, Au*L*α (pure metals), Fe*K*α, S*K*α (FeS_2), and Pb*L*α (PbTe). Additional corrections for peak overlaps (*e.g.*, Pd*L*α and Ag*L*α) were made. A Cameca Camebax electron microprobe was operated at 20 kV and 15 nA; the X-ray lines and standards were: Pd*L*α, Pt*M*α, and Pb*M*α (pure metals, and PbS). The WDS electron-microprobe analyses of silicate minerals and Cr–Fe–Ti oxides were carried out using a JEOL–733 microprobe. The operating conditions were 15 kV and 15 nA, and the following X-ray lines and standards were used: Si*K*α, Ca*K*α (wollastonite), Mg*K*α (periclase), K*K*α (orthoclase), Na*K*α (jadeite), Al*K*α (synthetic Al_2O_3), Ti*K*α (rutile), Fe*K*α, Cr*K*α, V*K*α, Ni*K*α, Mn*K*α (pure elements), and Cl*K*α (KCl).

Quantitative energy-dispersion (EDS) electron-microprobe analyses of various PGM, base-metal sulfides and silicate minerals were carried out at 15 kV and 1.7 nA, using a JEOL JSM–6400 scanning-electron microscope (SEM) equipped with a LINK eXL energy-dispersion spectrometer. The following set of standards was used: Pt, Ru, Os, Ir, Pd, Au, Ag (pure metals), Rh (synthetic RhSb), Co, Ni, Cu, Fe, Pb, Bi, S (pure elements, $CuFeS_2$, and FeS_2), Te ($PtTe_2$), and As ($PtAs_2$). The *M* X-ray line was used for Pt, Ir, Au, Pb, and Bi. The *L* line was used for Pd, Ru, Rh, Ag, Sn, Te, and As. The *K* line was used for Fe, Co, Ni, Cu, and S. The spectra were processed by a LINK ISIS on-line program. The counting periods were 100 s, and a finely focused beam (*ca.* 1 _m) was used in all of the SEM–EDS analyses. The *K*α line and the following set of standards were used for silicate minerals: SiO_2, apatite, MgO, orthoclase, jadeite, Al_2O_3, KCl, and pure Ti, Fe, and Cr.